Mu2e: Tracker and calorimeter study in MARS

(With focus of study on geometry and simulation)

Christina Ann Nelson
University of Hawaii at Manoa

Science Undergraduate Laboratory Internship (SULI) Program
Fermi National Accelerator Laboratory
Batavia, Illinois 60510

August 11, 2014

Mu2e is an experiment at Fermilab that will search for charged lepton flavor violation (CLFV) at an increasing sensitivity that will be able to probe equivalent energies as high as 10 000 TeV. The CLFV that will be sought is the neutrino-less conversion of a muon into an electron in the vicinity of an aluminum nucleus. This process has a very low probability, 10^{-54}, in the Standard Model (SM) of physics, yet discoveries of neutrino oscillations since the development of the SM, and more, lead more than one reason to point to theories beyond the Standard Model that account for CLFV, some of which have already been proven. The focus of this study is on the development of MARS15 models of the tracker and calorimeter that will be used to detect the conversion electrons, specifically on the geometry and simulation in the MARS code. Geometrical models created with the purpose of ignoring backgrounds as much as possible, coupled with measuring particles momenta, trajectory, and end energy are the main strengths employed to detect our goal. Absorbed doses in the tracker and calorimeter by background electrons and other particles are simulated. Results are discussed and data given of a toy model simulation and a full model simulation in MARS.

Table of Contents

I. Mu2e INTRODUCTION / OVERVIEW

A. What is Mu2e and what are its motivations?

Mu2e is an experiment at Fermi National Accelerator Laboratory that looks for an ultra-rare process: the neutrino-less conversion from muons to electrons. Neutrino-less muon to electron conversion is known as lepton flavor violation (LFV). In the Standard Model (SM) of physics this ultra-rare conversion process is predicted to happen at a rate of less than 10^{-50}. Beyond the standard model (BSM) theories predict the conversion rate to occur at approximately 10^{-16}. From the Standard Model, lepton flavor conservation exists in a presumption that the neutrinos have zero mass[1]; since then, there has been the discovery of neutrino oscillation, thereby giving rise to the conclusion that the neutrino has some mass. Neutrino oscillation violates lepton flavor conservation, which is a crack in the SM and clearly a pointer to new physics. Naturally after discovering LFV in neutrinos, one would look for CLFV in heavier particles like the muon; one would investigate the muon before the heavier tau particle because heavier particles imply probing to higher energies ($E = mc^2$).

The Mu2e experiment aims to increase the sensitivity, and thus the limit of experiment to be able to probe energies a high as 10 000TeV. By running the experiment for three years of data acquisition (DAQ), optimization for detecting this ultra-rare process can be maximized. From figure 1, previous experiments in search of CLFV have an upper limit of 1000 TeV. Preceding experiments have a limit of: MEG: ~1100 TeV, SINDRIUM-II: ~1000TeV, and MEGA: ~400 TeV[1]. As stated, in the Mu2e conceptual design report (CDR), the sensitivity will be 10^{-16} and is aimed at increasing the sensitivity by a factor of 10 000 better than that of current experimental limit. This is done by " using a bunched proton beam slow-extracted…An experimental setup consisting of high-field pion capture solenoids, curved solenoids to select beam momenta, and a

curved solenoid spectrometer to detect muon to electron conversion with low-counting rate conditions...To improve the sensitivity several important features are considered: 1.) Highly intense muon source, 2.) Pulsed proton beam 3.) Muon transport with curved solenoids 4.) Spectrometer with curved solenoids" [1]

FIG 1: Previous experiments in search of CLFV and their upper limits compared to Mu2e [8].

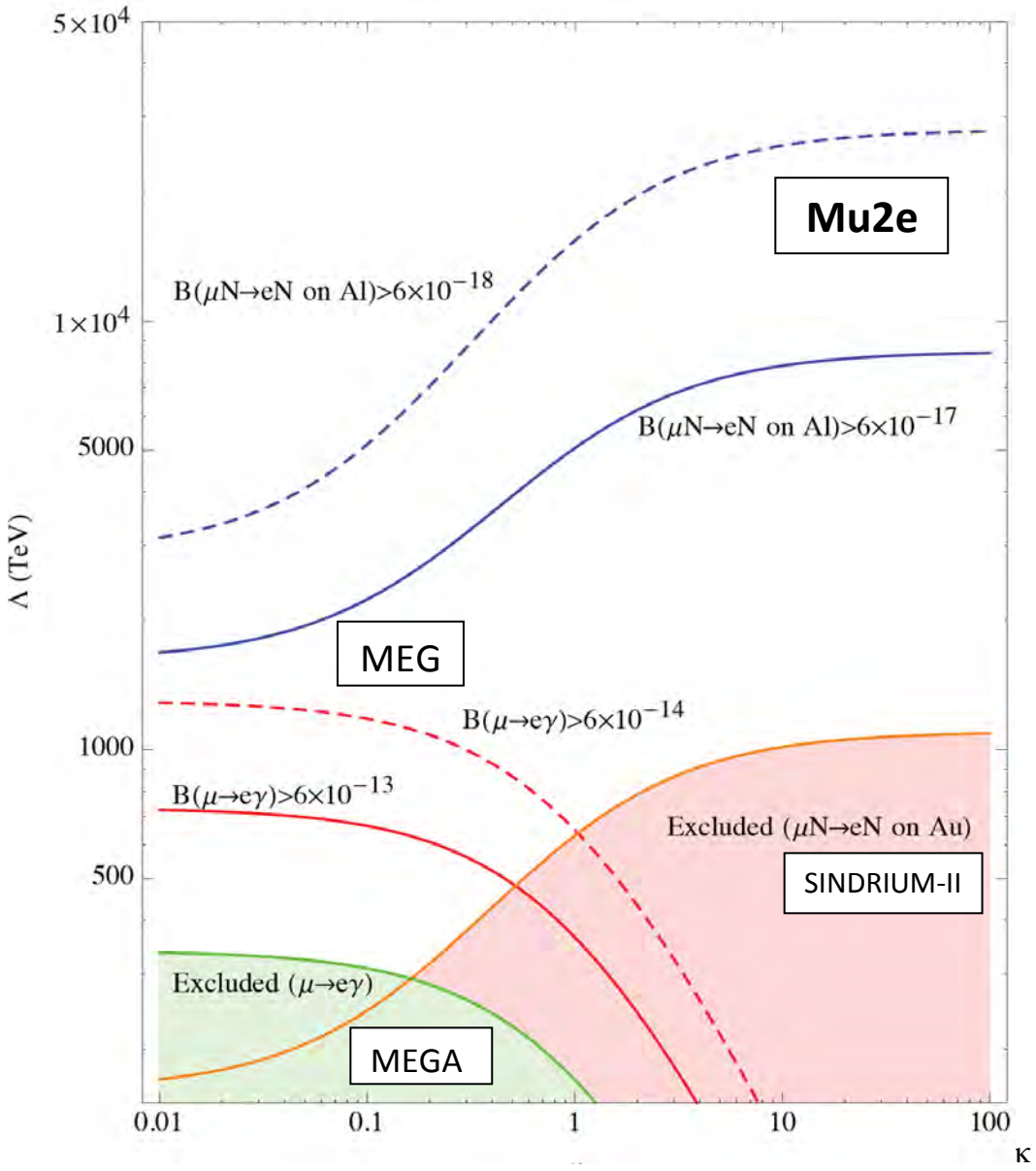

B. Apparatus development: focus of work

The design of the detector is of significant importance to Mu2e and that is the focus of this work, particularly the tracker and the calorimeter in the detector solenoid of the experiment. The geometrical design and materials that make up the tracker and calorimeter must be created with optimizing the ability to detect the conversion electrons of ~105 MeV. There occurs in this experiment, to say the least, significant background, which can over-dominate, mimic, and cloud the detector's ability to recognize the conversion electron. Some of the dominant backgrounds are: decay in orbit (DIO): 53%; radiative muon capture (RMC): 14%; beam electrons: 9%; and muon decay in flight: <7% .[1] The methods for subverting these backgrounds as best as possible in the detector solenoid are to set up the working time window after 700 ns, and [2] (the study done here specifically), to use constant magnetic fields and specific geometrical design to ignore particles without the conversion energy (CE). The tracker will measure the momentum and trajectory, while the calorimeter will measure the energy before the particle reaches the beam stop; the combination of this data will optimize the ability for Mu2e to detect this ultra-rare process.

FIG. 2: Working window set up 700 nanoseconds after proton on target (POT) pulse.

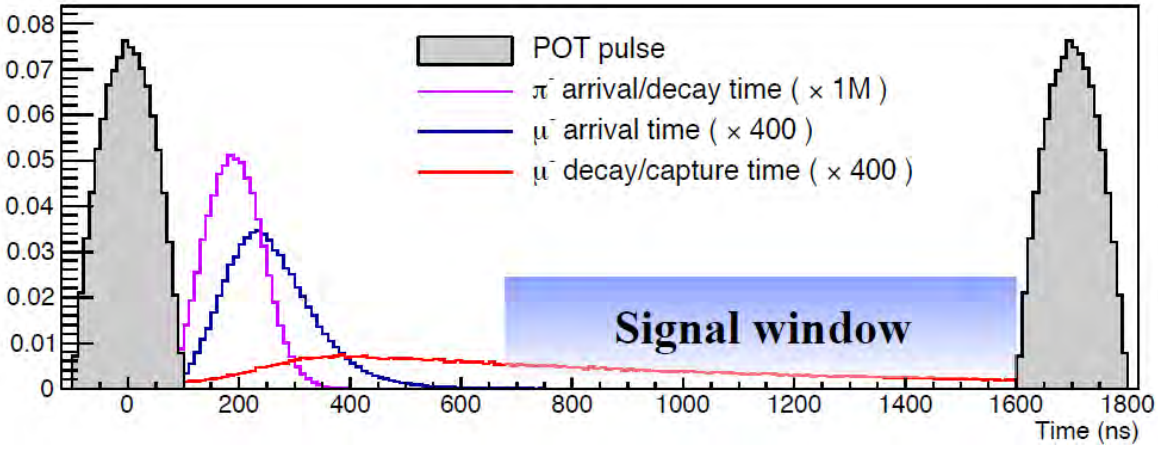

Compared to previous simulations, many of which are in GEANT4, this study will be done in the MARS code developed by Nikolai Mokhov[3]. The geometry of the tracker and calorimeter have been developed in ROOT from scratch based upon the latest design in the CDR. Two different designs for the tracker are implemented, a more detailed and specific tracker is tested in a MARS toy model observing single particle interaction, while a simplified version is tested in a MARS full model and simulation. Magnetic field gradients deciphered from a field map were inputted into the MARS toy model, while the existing magnetic field functions were left untouched in the full MARS model and full simulation. Materials for the tracker and calorimeter were also inputted into the MARS material file, this information was obtained from the CDR and inputted as atomic weight, atomic number, weight fractions, and total density The data from these simulations will provide comparison and insight that will contribute to studying the background energy limit readings of particles in the detector solenoid, and energy deposition in the tracker and calorimeter. (Reconstruction of particle's path algorithm is in the process of development in MARS) This is important as a proof of concept for Mu2e in mainly two ways that the results will address: first, to show optimization of our ability to detect the conversion electrons and second, to prove that the experiment is able to physically last the three year duration needed to run the pulsed proton beam.

II. THEORETICAL & EXPERIMENTAL TALK ON MU2E

A. Mathematical reference

$$\mu^- N \rightarrow e^- N$$

Mu2e, using high precision measurements is searching for CLFV, which is the neutrino-less conversion of a muon into an electron in the vicinity of a nucleus [2]. The importance for investigating CLFV with high intense slow muons is practical and independent if the Large Hadron Collider (LHC) finds Supersymmetry (SUSY) or not; because either way, finding CLFV in muon to electron neutrino-less conversion will naturally extend from SUSY found at the LHC, or reveal SUSY at levels of higher energy that the LHC cannot reach[1]. Stated earlier, CLFV normally forbidden in the standard model. When one does account for neutrino mass, neutrino oscillation can be expressed in the SM through oscillation loops[6]. The process in the SM is predicted to happen at a "rate proportional to $(\Delta m_{ij}/M_W)^4$, where delta mij^2 is the mass difference squared between ith and jth neutrino mass eigenstates, and Mw is the mass of the W boson"[2]. Loops are suppressed over the sums of the squared ratios stated above. Using measurements of θ_{13} and calculating for the $\mu \rightarrow e\gamma$ decay Marciano et al (2008) finds[6]:

$$\mathcal{B}(\mu \rightarrow e\gamma) = \frac{3\alpha}{32\pi}\left|\sum_{i=2,3} U^*_{\mu i} U_{ei} \frac{\Delta m^2_{i1}}{M^2_W}\right|^2 \sim 10^{-54},$$

This is the rate of muon to electron with a photon conversion predicted in the SM.

There are new physics models that accounts for neutrino mass and predicts this rate instead to be 10^{-16}, such as super symmetry via slepton mixing, sea saw models of heavy neutrinos, and Higgs doublet models to name a few[6]. CLFV searches will help to narrow down the options for BSM models and provide parameters. The main way that Mu2e will contribute to a deeper understanding of SUSY or other BSM models is with increased sensitivity. "Among these the μ^- N$\rightarrow e^-$ N process has sensitivity to the broadest array of NP models" [2].

Effective CLFV can be expressed in the Lagrangian equation (interpolating polynomial):

$$\mathcal{L}_{\mathrm{CLFV}} = \frac{m_{\mu}}{(\kappa+1)\Lambda^2}\bar{\mu}_R\sigma_{\mu\nu}e_L F^{\mu\nu} + \mathrm{h.c.} + \frac{\kappa}{(1+\kappa)\Lambda^2}\bar{\mu}_L\gamma_{\mu}e_L\left(\bar{u}_L\gamma^{\mu}u_L + \bar{d}_L\gamma^{\mu}d_L\right) + \mathrm{h.c.}$$

Robert Bernstein explains the Lagrangian excellently:

First term = the "loop" (or magnetic moment operator)

Second term = "contact" term operator

h.c. = hermitian conjucate

Bernstein goes on to explain: "SUSY belongs with the first term and that particle exchange is reflected in the second. The coefficients of the two types of operators are parameterized by two independent constants: Λ Λ, the mass scale of the new physics, and κ κ, a dimensionless parameter that mediates between the two terms. L L and R R indicate the chirality of the different Standard Model fermion fields, $F^{\mu\nu}$ $F\mu\nu$ is the photon field strength and m_{μ} $m\mu$ is the muon mass. This Lagrangian coupling quarks to leptons will govern $\mu N \to e N$, $\mu \to e\gamma$ and $\mu \to 3e$ in many models"[6].

Magnetic moment type operator

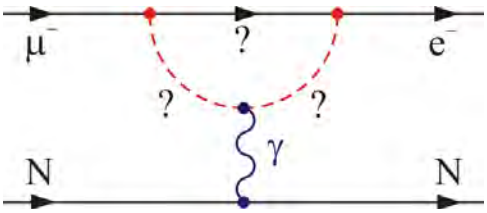

κ << 1

Contact term operator

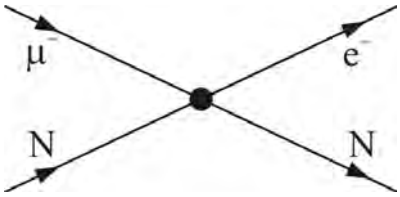

κ >> 1

FIG 3: Visually we can view the first term as the drawing on the left, and the second term as the drawing on the right of the Lagrangian expression put forth above.

B. What the Mu2e experiment will measure

Mu2e will measure the ratio of muon to electron conversions to the number of muon captures by the Al nuclei:

$$R\mu e = \Gamma(\mu^- + (A, Z) \rightarrow e^- + (A, Z)) \;/\; \Gamma(\mu^- + (A, Z) \rightarrow \mu + (A, Z-1))$$

Muons in the 1s sate around the Al nucleus predominantly: 1.) Decay via the weak interaction into an electron and two neutrinos, this is known as decay in orbit (DIO): $\mu^- \rightarrow e^- \bar{\nu}_e \nu_\mu$ 2.) Undergo radiative muon capture (RMC): $\mu^- N \rightarrow \gamma \nu N'$ which leads to nuclear breakup. RMC produces ejected protons from the nuclear breakup, which is a source of noise, but the signal does not mimic 105 MeV. On the other hand, DIO produces electrons that are also 105 MeV which are reflected in the tail end of the Michel peak. Therefore our only way of differentiating these DIO electrons from the conversion electrons is by momentum and trajectory recorded in the tracker[4].

FIG 4: DIO recoil tail is a dominant source of background because of the same energy emitted by the electrons[4], this contributes to approximately 60% of background as stated in the CDR

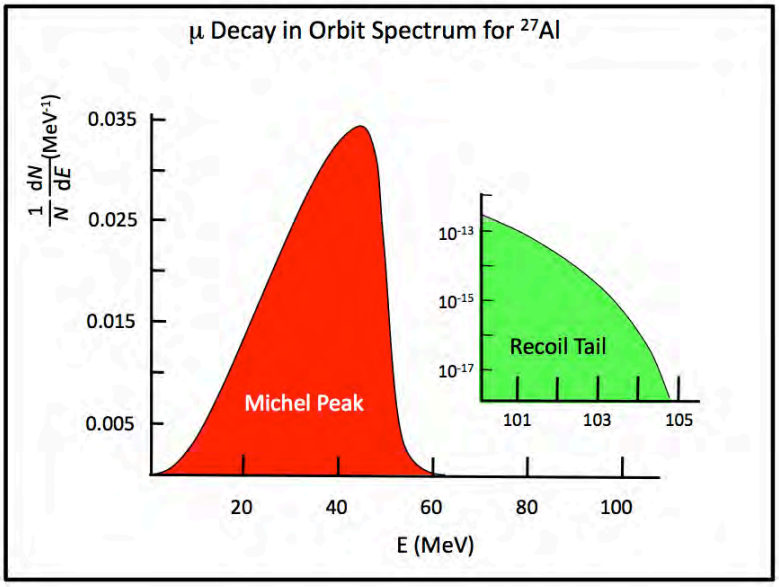

III. TRACKER DESIGN & BUILDING FOR SIMULATION

The tracker provides the primary momentum measurement for conversion electrons.[4] The Mu2e tracker sits surrounded by a superconducting solenoid with a uniform magnetic field of 1 Tesla. The tracker is situated in the experiment to operate in the optimal working time window of $670 < t < 1\ 595$ ns, where $t = 0$ is the arrival of the peak beam pulse at the aluminum stopping target.[4] Also, before the particles reach the stopping target, selected particles with determined momenta and negative charge will be selected in the transport solenoid. In order to study backgrounds, the tracker will need to work in the time window of $500 < t < 1700$ ns.[4]

A. Geometry study and building

The geometrical design of the tracker is built in ROOT with the intention to measure conversion electrons, while ignoring other particles having less momentum. The tracker has an inner radius of 390 mm, which is positioned in order to not intersect with a traveling electron with energy less than the conversion electron energy (CE) of 105 MeV. Two designs were built and studied. A simplified version of the tracker from the conceptual design report (CDR) with twenty discs that has an outer radius of 700 mm, a thickness of 40 mm and an inner cut out shape of a twelve-sided polygon making the inner radius 390 mm. The other design studied models the CDR tracker more accurately and is made up of rotated trapezoidal panels. Three trapezoids are rotated 120 degrees relative to one another, forming an inner shape of a triangle; this is called a plane. Two planes are placed front to back and the back plane is rotated sixty degrees relative to the front; this makes up a panel. Then two panels are placed front to back with the back panel rotated 30 degrees relative to the front, this creates one station. The tracker is then comprised of twenty stations. The overall shape has an outer radius of 700 mm and an inner radius of 390 mm. In order to model the straws that create the panels, divisions along the y and z direction were

coded in accurate number, 100 straws per trapezoid; 2 rows of 50 divisions. The geometry for the tracker is written in ROOT, which is a C++-like language and placed into the tgeo_init.cc file in the mars15 directory. (Source code for geometry is viewable in Appendix)

FIG. 5: Simplified tracker YZ plane.
(L to R: Stopping target, tracker, calorimeter)

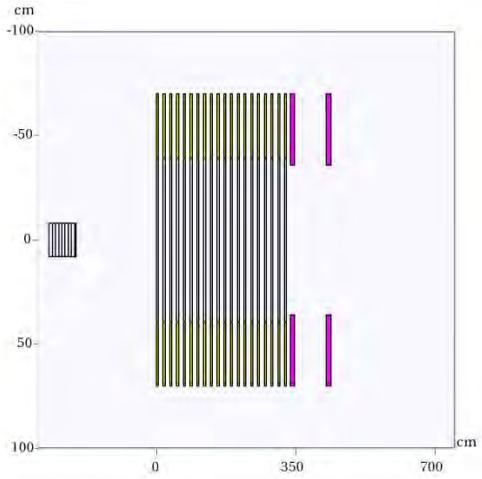

FIG. 6: Simplified tracker XY plane.

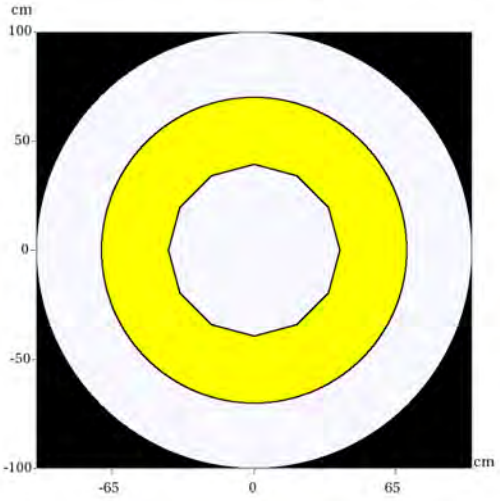

FIG. 7: Tracker design with trapezoid panels YZ plane, from L to R, stopping target, tracker, calorimeter.

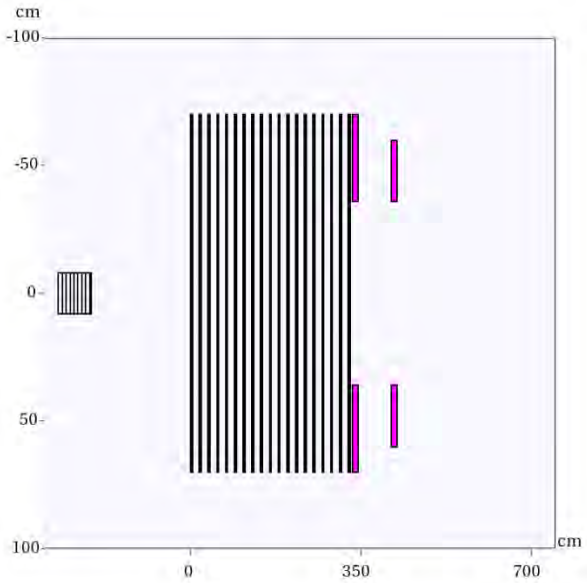

FIG. 8: Tracker design with trapezoidal panels XY direction; view panel rotation creating one station.

(Note: Division segments upon zoom are evenly spaced, and the corners of panels do not touch.)

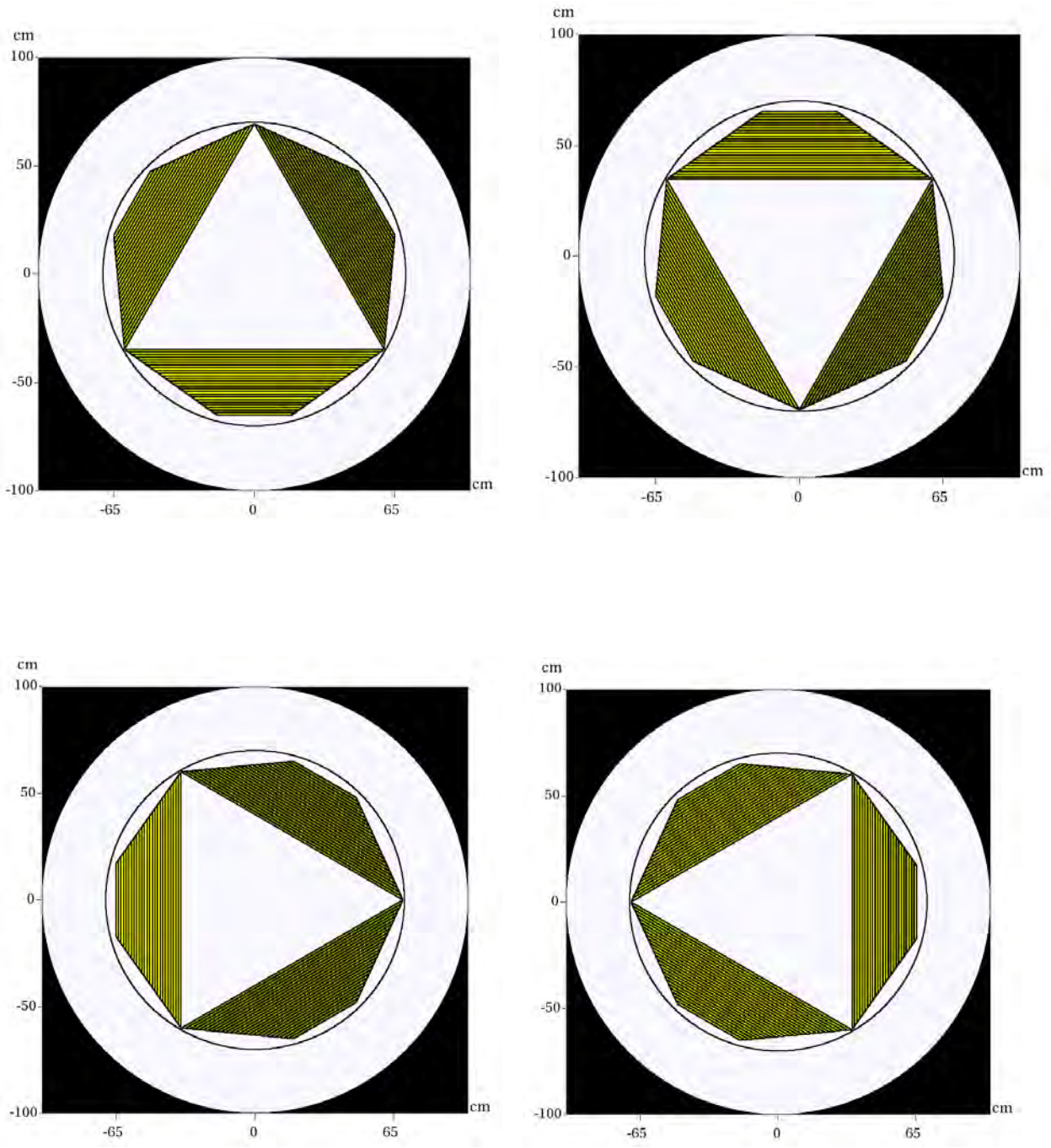

FIG. 9: Corner of trapezoidal tracker model in zoom, it is important to show that the geometry does not overlap because overlapping geometry in MARS will yield inaccurate results in simulation.

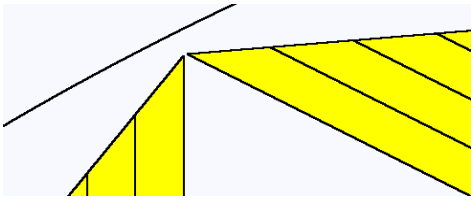

FIG. 10: Assembled tracker from CDR.

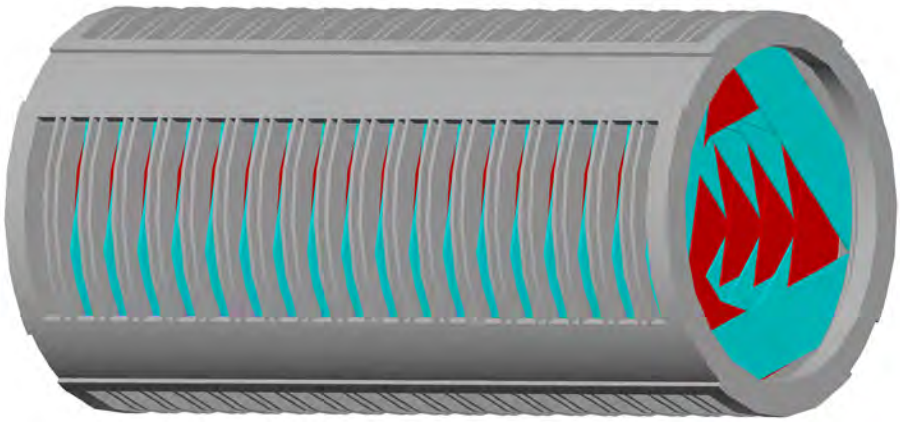

B. Materials study and input

The tracker design consists of low-density array of straw drift tubes filled with 80:20 argon and carbon dioxide gas. The gas will ionize thus detecting an electron. The straw contains a 25μm sense wire inside a 5mm diameter tube made of 15μ thick metalized Mylar. As stated in the CDR, the straw design was chosen because the straws work consistently in zero to one

atmosphere pressure differential, the design assists in need for repairs, and the transverse design places support, electronic readout, cooling and gas at a large radii which reducing cross talk and interference[4]. The tracker will have approximately 20 000 straws throughout the 20 stations and each station will provide approximately 200μm of measurement of track position[4]. In order to input the materials into the MARS material input file, the per cent density of each material was calculated and defined in the MATER.INP file and placed into a card that MARS will read into the program.

Figure 8: The input 'Mix1' is the mix of all materials making up the tracker placed in MATER.INP

'MIX1' average density: 0.31806 Number of elements: 6

Atomic Weight	Atomic Number	Weight Fraction
39.94800	18.00000	0.79200
12.00700	6.00000	0.06613
15.99900	8.00000	0.13226
183.40000	74.00000	0.00500
26.98000	13.00000	0.00018
197.97000	79.00000	0.00009

One will note here that upon inspection, I did not include Mylar in the input card. This is a mistake in the weight fractions, but the average density when I recalculated is 0.316 g/cm^3, which is approximately a 1% difference. This may effect the results in reading power deposition and particle interaction with the tracker.

C. B field study

In order to input the magnetic field into the toy model, a B field study was done in order to find the gradients at positions throughout the detector solenoid reading in the magnetic field map file. The detector solenoid consists of the aluminum stopping target of sixteen foils. Positioned longitudinally 2 100 mm downstream from the stopping target is the tracker, and 80 mm longitudinally from that are the two calorimeter rings separated by 800 mm. The magnetic field from the stopping target to the tracker decreases linearly from 1.5 Tesla to 1 Tesla upon reaching the tracker.[4] Through the tracker the magnetic field is approximately linear, although at very small scales there is small nonlinearity, which overall oscillates in a range of 0.5% deviation from 1 Tesla. From the tracker through the calorimeter the magnetic field linearly decreases again. In order to find the function for the gradients of these fields, ROOT was used to do a linear fit on the graph and then the functions were inputted into bcalc.cc file in mars15 directory. Please note that the gradient found is a very rough approximation because only about eleven points were plotted to determine the gradient function. This study was done more as an exercise in the toy MARS model to observe how the magnetic field determines a particles trajectory and therefore how it interacts with the geometry of the tracker and calorimeter. One would expect this rough approximation to diverge more quickly and greatly as one moves away from the center of the detector solenoid than in the full MARS model.

FIG. 11: Magnetic field function through the detector solenoid.
Middle of stopping target to entrance of tracker: 5 946 cm – 7 956 cm
Through the length of tracker: 7 956 cm – 12 946 cm
From exit of tracker to exit of calorimeter: 12 946cm – 15 946 cm

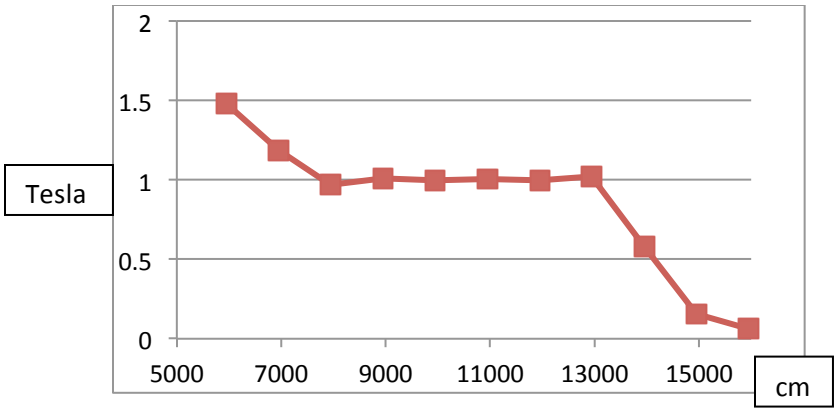

FIG. 12: Magnetic field in the tracker, 1 Tesla; there are some asymmetries (note scale).

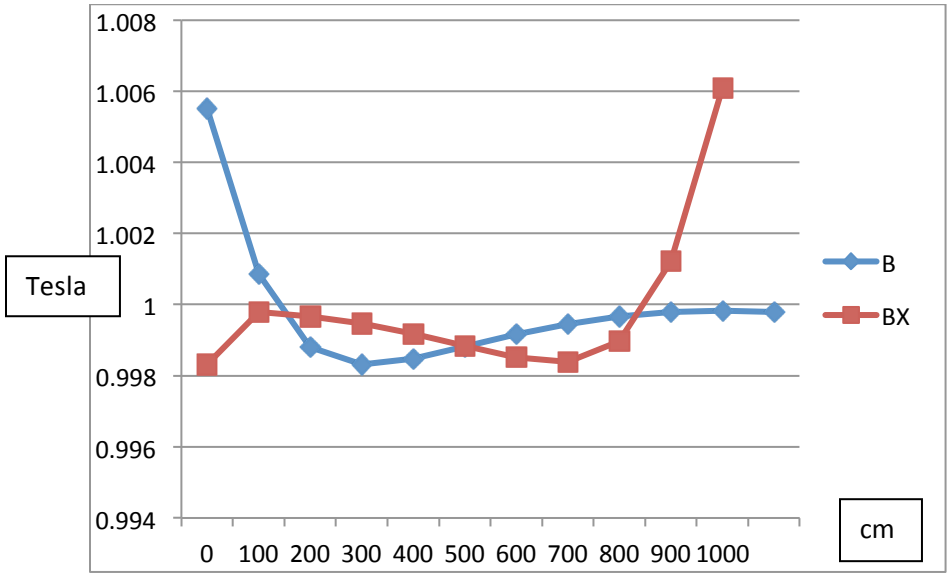

FIG. 13: YZ plane of detector with B field. (Simplified model in MARS toy model)

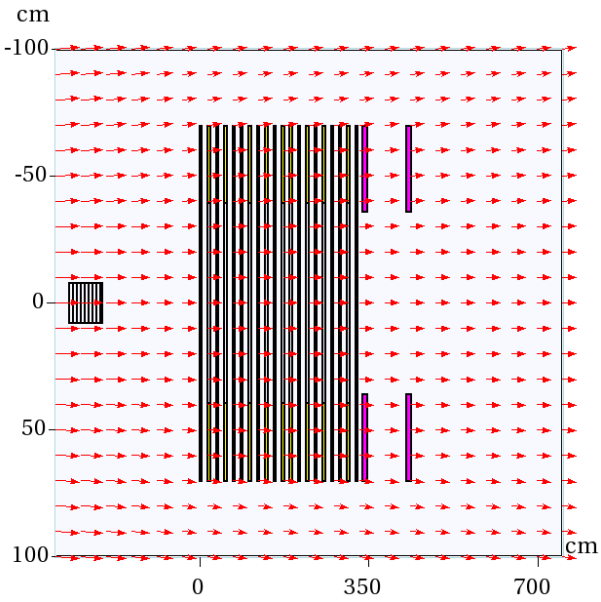

FIG. 14: XY plane of tracker with B (Simplified model in MARS toy model)

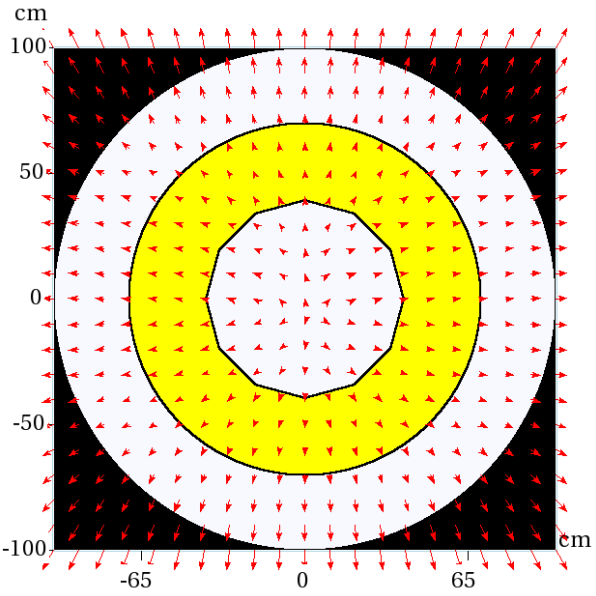

IV. CALORIMETER DESIGN & BUILDING FOR SIMULATION

In the Mu2e experiment, upon entering the detector solenoid, the particles first hit the aluminum stopping target; then travels through the tracker and finally reaches the calorimeter. The calorimeter is where the particle's energy will be acquired. Finally, the particle will proceed to a beam stop. The calorimeter has the concern of measuring false conversion electron energy due to accidental hits combining with lower energy particles and stemming from pattern recognition errors in the overwhelming amounts of hits it will be receiving. To rectify this concern, the calorimeter will read redundant measurements and couple this information with data from the tracker. Also, the calorimeter has the function of providing trigger to the experiment.[4]

A. Geometry

The current geometrical design for the calorimeter is a pair of discs with an inner radius of 360 mm, an outer radius of 700 mm for the front disk, and 600 mm for the back disk, with a thickness of 110 mm. The first disk is to be placed longitudinally 80 mm from the exit of the tracker, and the second disk 800 mm behind the first disk. According to the CDR, the disk configuration produces an efficiency of 84%, which is a substantial gain compared to the 78% efficiency of the prior vane model.[4]

B. Materials

The material that makes up the calorimeter is especially important to study in order to prove that it will not decay, melt, or break down in the required three year period that Mu2e will need to run in order to acquire enough data for decent analysis. The latest design material for the calorimeter from the CDR consists of LYSO crystals that have been studied in the field of detectors greatly.[4] Similar to the tracker, the LYSO material was inputted into the MATER.INP file and inputted as a card in MARS.

FIG 13: The input 'LYSO' placed into the MATER.INP file

Card 4 'LYSO' Average Density: 7.28 Number of elements: 4

Atomic Weight	Atomic Number	Weight Fraction
174.96680	71.00000	0.68645
88.90584	39.00000	0.02934
28.08500	14.00000	0.06876
15.99900	8.00000	0.16681

V. SIMULATION

A. Single particle simulation in MARS model: Results

To study the simulation in the toy MARS model we ran single particles such as one electron, one muon, one pion, and one positron through the detector, starting from the middle of the stopping target to see if the particle interacted and moved as we expected it to. The toy model only consists of the aluminum stopping target, the tracker, and the calorimeter in a vacuum. The results are shown in the following figures for an electron with energy of: 44 MeV, 60 MeV, and 105MeV. Here we are looking to confirm that as the particle spirals through the tracker, the geometry is ignoring backgrounds of electrons that have a momentum of less than 105 MeV/c. Upon simulations, it was found the muon, pion, and positron will have less momentum, or energy than the electron, therefore they will not generally produce dominant backgrounds through DIO or RMC, so we will focus on the electrons in the toy model. An electron with 44 MeV, kinetic energy, clearly spirals through the tracker without intersecting the tracker, but one can see from figure 12 that about half-way through the tracker the electron disappears. After investigating why, it was found that the ALMX physics control in MARS was set to measure too small of a step on the magnetic field for single particle interaction, the magnetic field steps were basically running out of the array, but in the full simulation model this occurrence did not happen. From the MARS manual, ALMX calculates the maximal angles on a step due to a magnetic field and is allowed for the first five intervals magnetic field for five energy intervals _ = |E0 − E|/E0: <0.001, 0.001-0.01, 0.01-0.3, 0.3-0.99, >0.99. The single particle interaction had too low of an energy and made the incremental steps extremely small which in turn exceeded the array.

FIG. 15: 44 MeV electron moving from middle of stopping target through tracker and calorimeter, XZ direction.

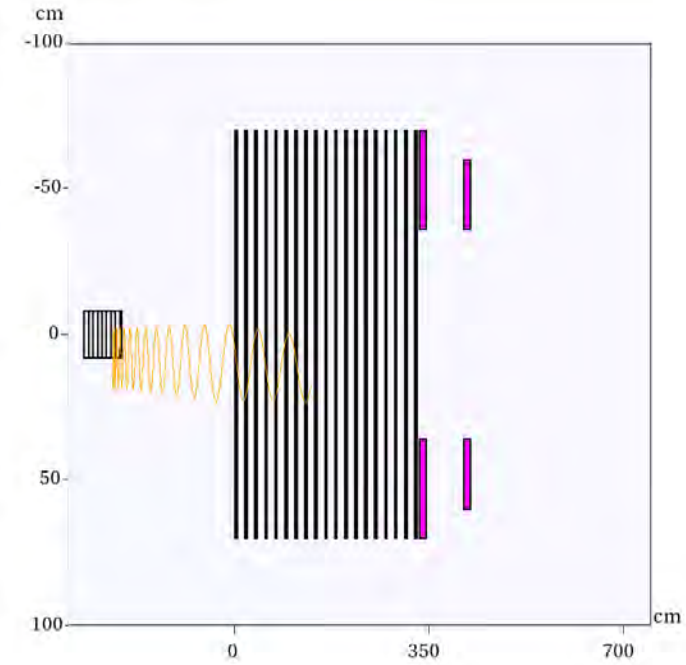

FIG. 16: 44 MeV in trapezoid tracker model XY direction.

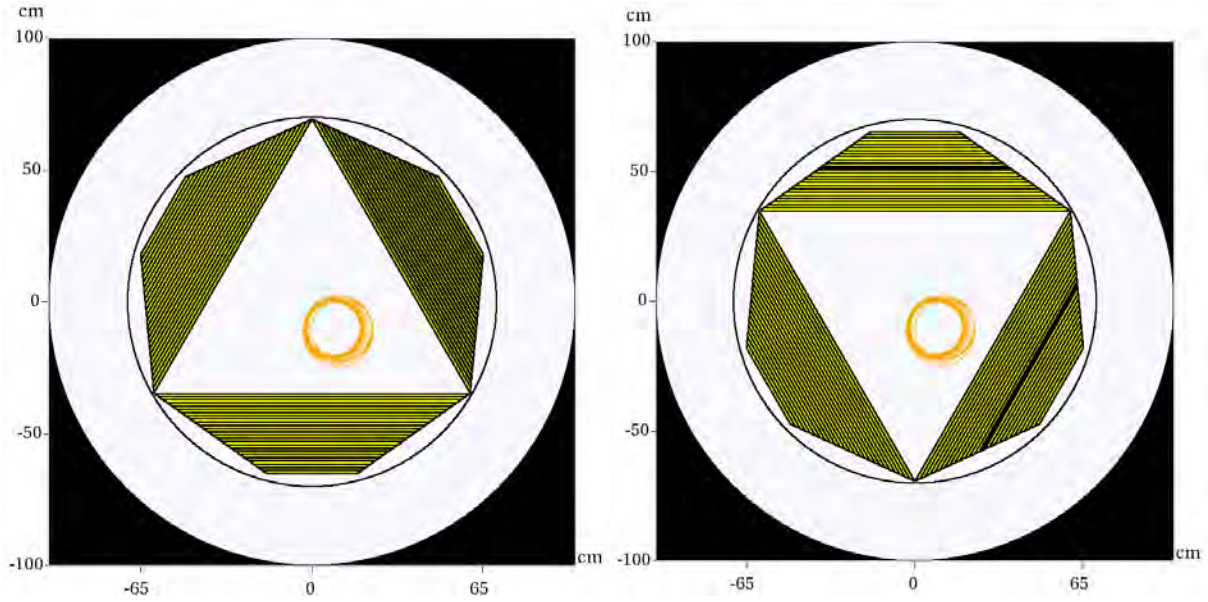

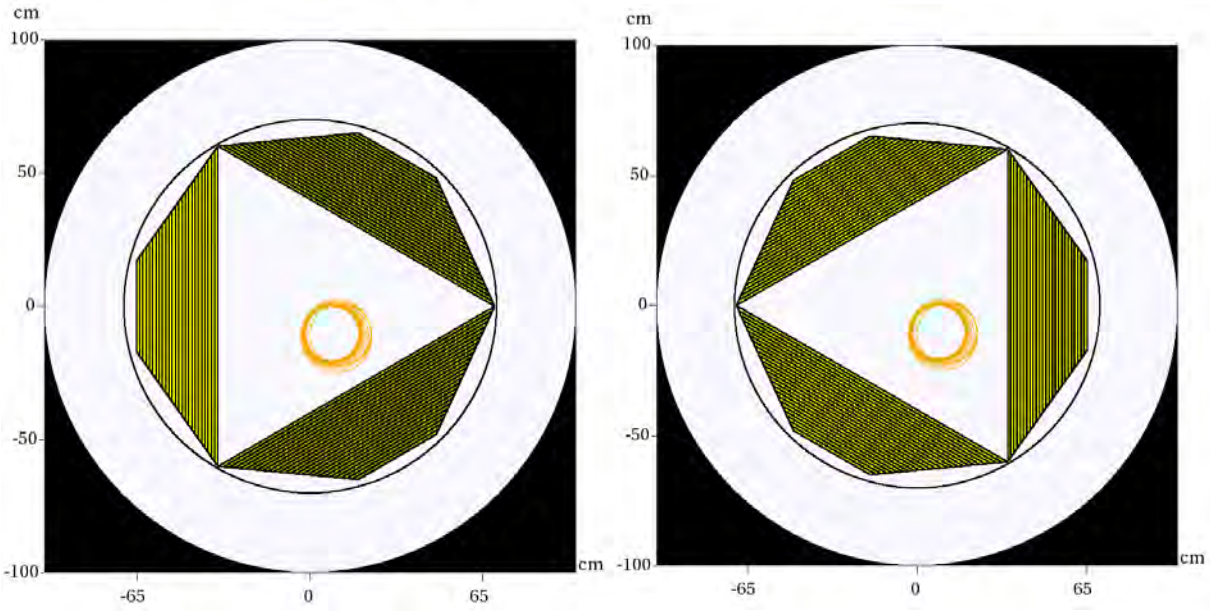

Never the less, we can still observe how the particles spiral through the detector solenoid and confirm if they intersect or not with the tracker. One expects a 60 MeV electron to not intersect with the tracker, but here it was found that in one run, the electron did not intersect with the tracker, but in a separate run, it is observed that the 60 MeV electron does indeed intersect with the tracker and in yet another run was observed to produce some photons upon reaching the calorimeter. Upon closer inspection it is found that in the toy MARS model when the direction cosines are: $\alpha = 0$, $\beta = 1$, $\gamma = 0$, 60 MeV electrons and 105 MeV electrons (44MeV electrons did not propagate far enough to observe this affect) tend to slope towards the –x direction. When the direction cosines are: $\alpha = 1$, $\beta = 0$, $\gamma = 0$, the electrons just mentioned slope in the –y direction. The direction cosines coupled with the rough approximation of the magnetic field gradient (as mentioned in the B field study section) function in the MARS toy model makes us observe the 60 MeV electron sloping too much and intersecting the tracker, which is what we don't want. This information shows that the direction the particle is ejected from the stopping target as well

as the magnetic field gradient determines if a 60 MeV electron will intersect with the tracker and become a source of background or not.

FIG. 17: 60 MeV electron in trapezoid panel tracker toy model, XZ direction.

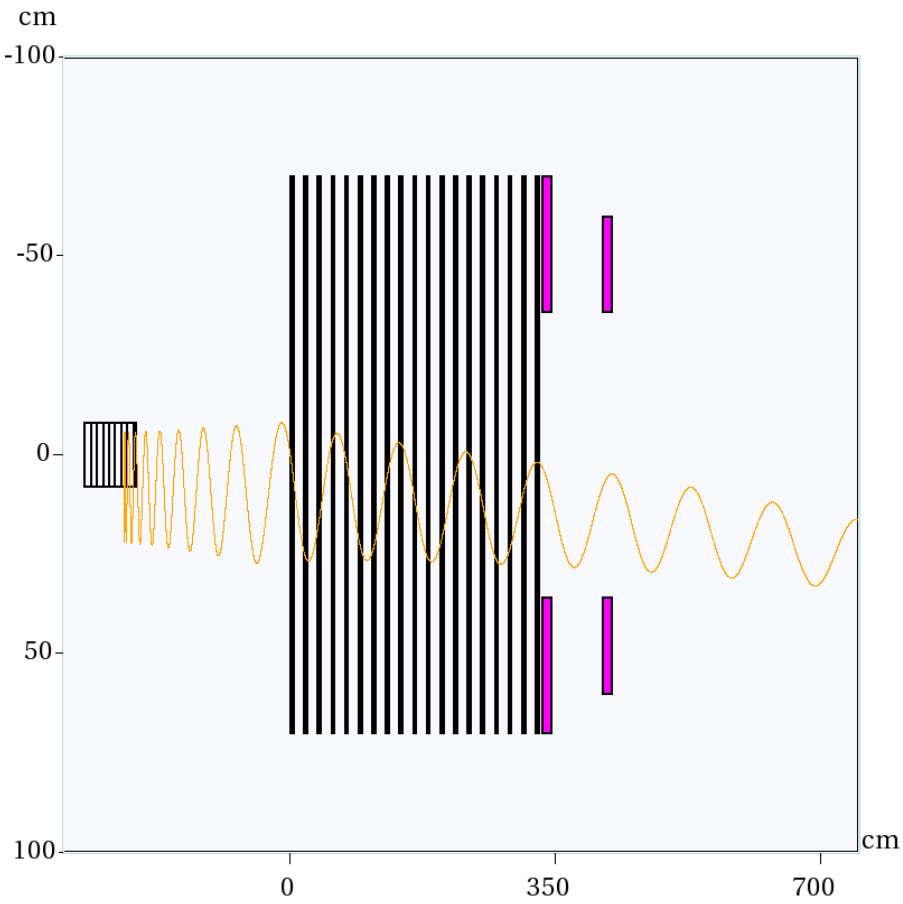

FIG. 18: 60 MeV electron traveling through tracker in XY direction

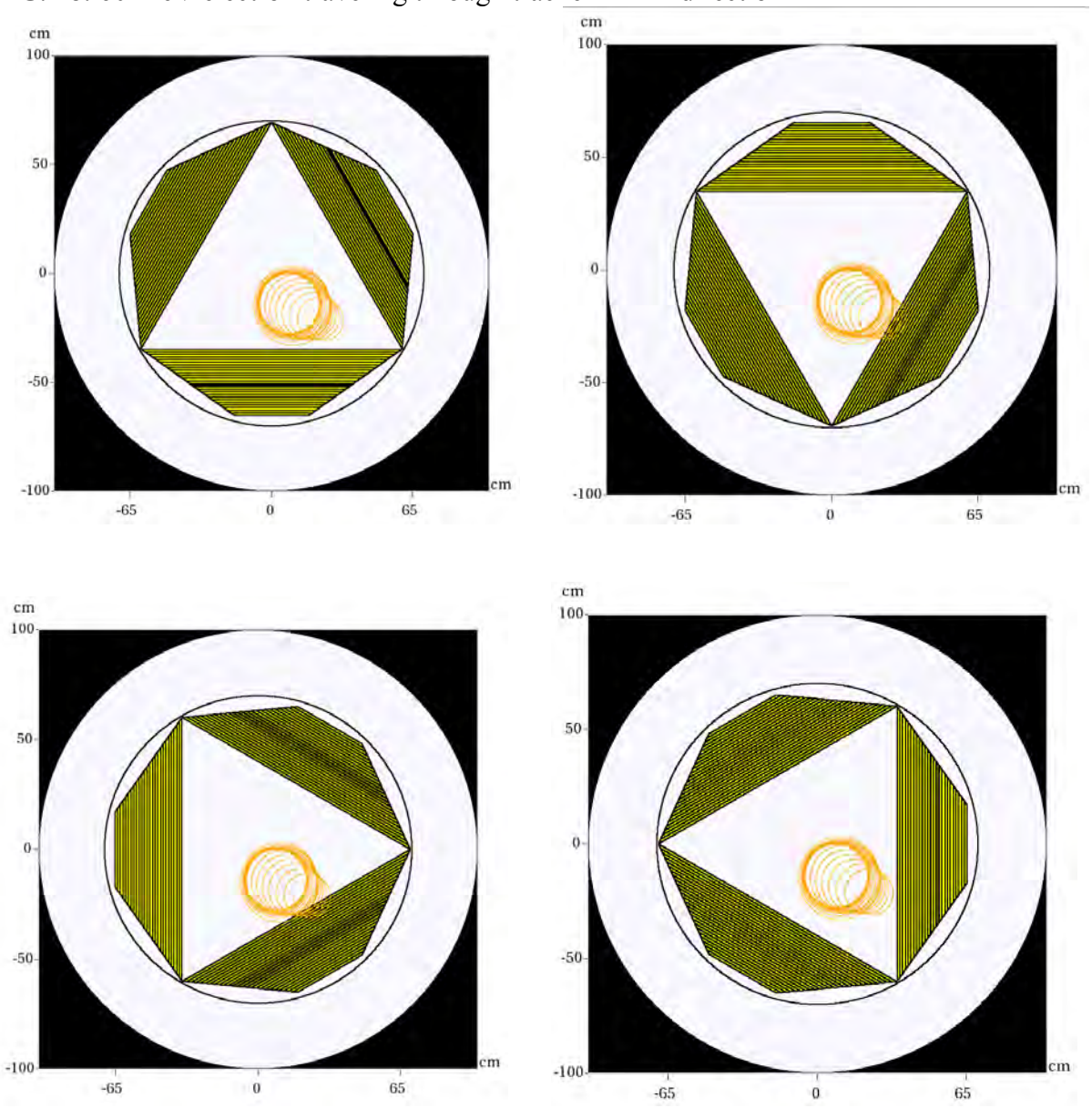

In figures 19 and 20 we are observing an electron with kinetic energy of 105 MeV that is sent through the MARS toy model from the middle of the aluminum stopping target. The particle propagates through the tracker and clearly intersects the tracker's panels and stations emitting photons. One can also observe that the radius of the oscillating electron with 105 MeV is larger than electrons with less energy, which is to be expected.

FIG. 19: 105 MeV electron moving through tracker; note the phtons that are emitted in blue due to interactions with the tracker. XZ direction.

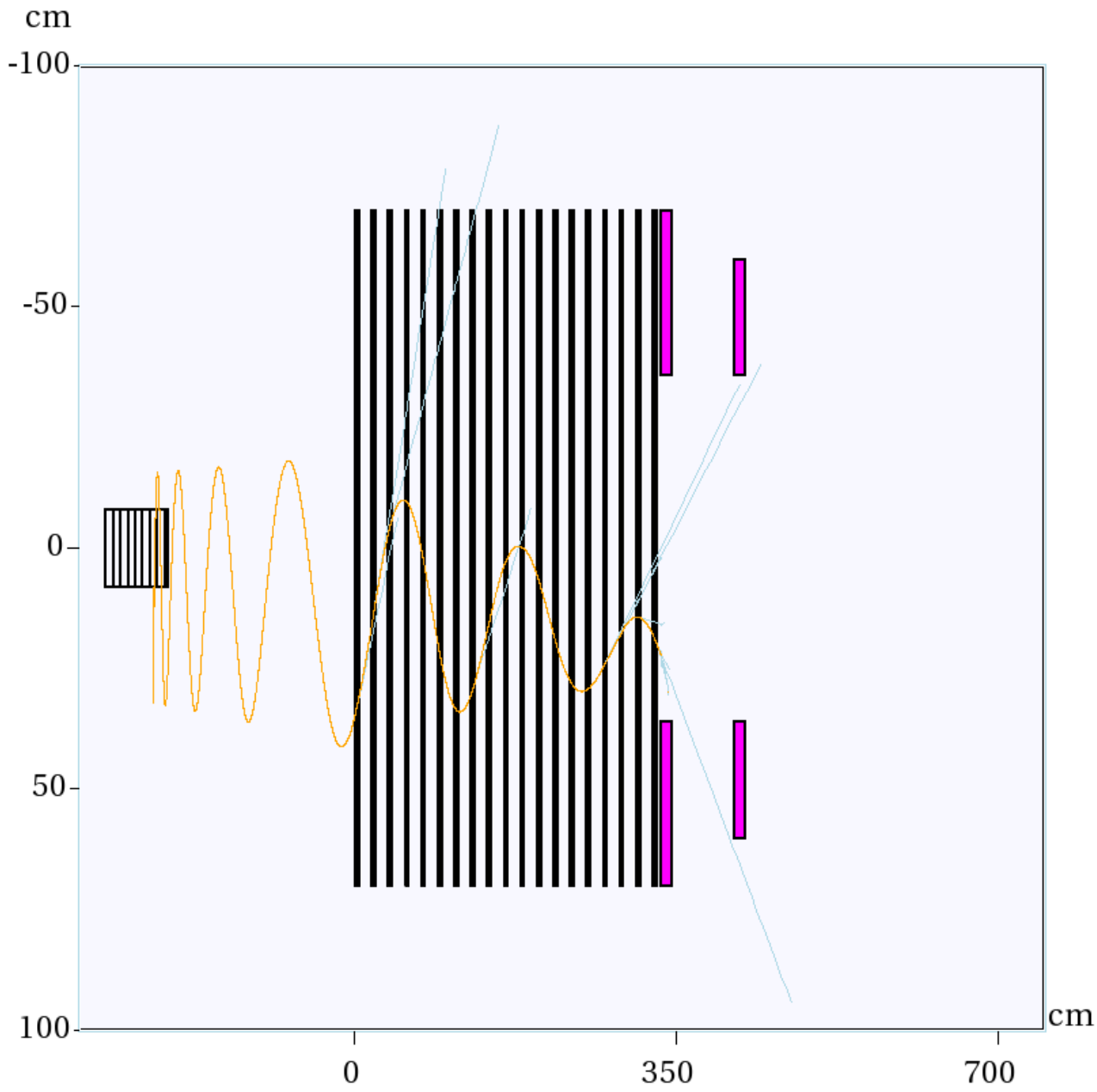

FIG. 20: 105 MeV electron sent through trapezoid panel tracker in toy model. XY direction.

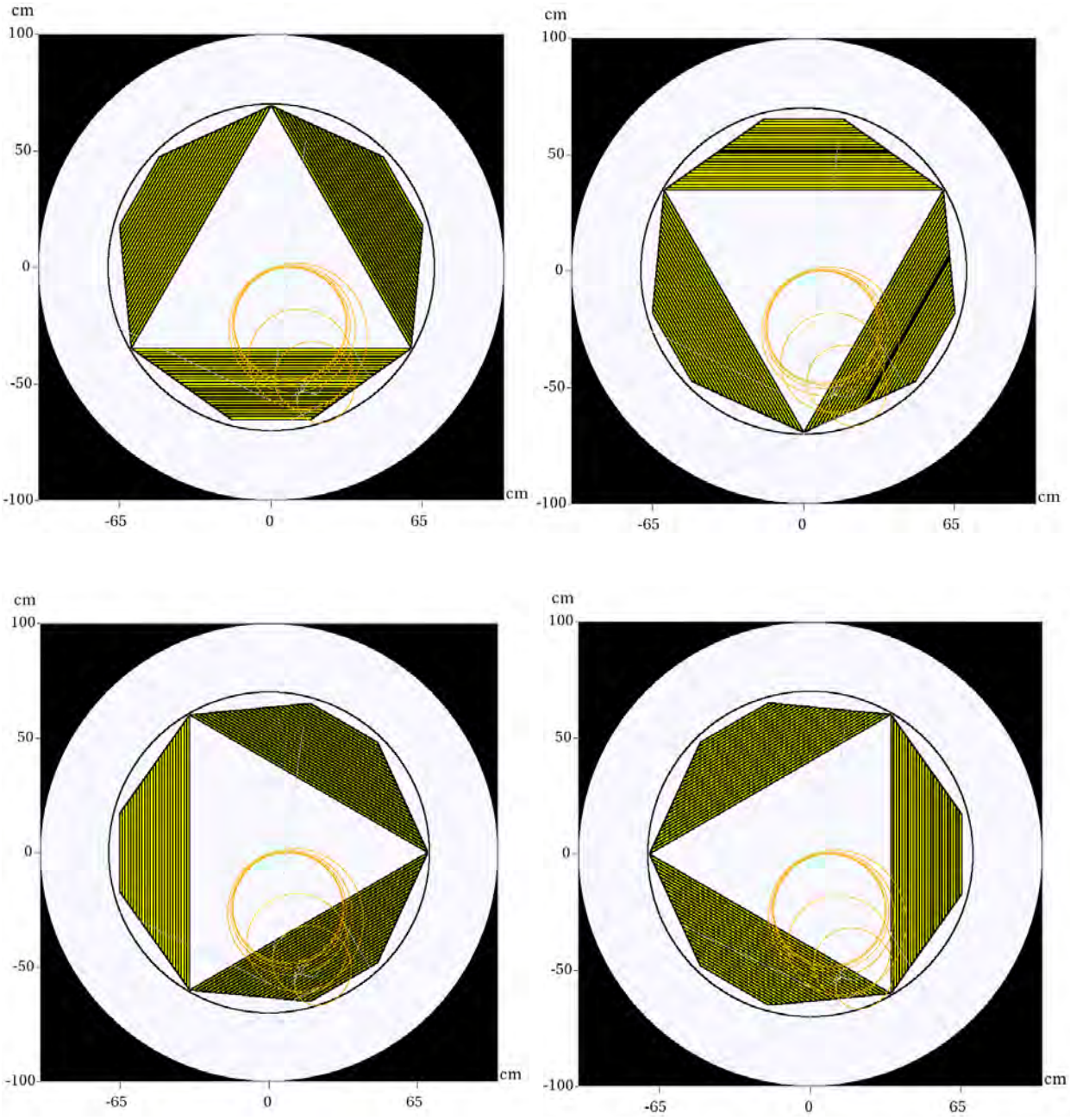

FIG. 21: Toy MARS model with simplified Geometry design 105 MeV single electron sent through detector, XZ direction

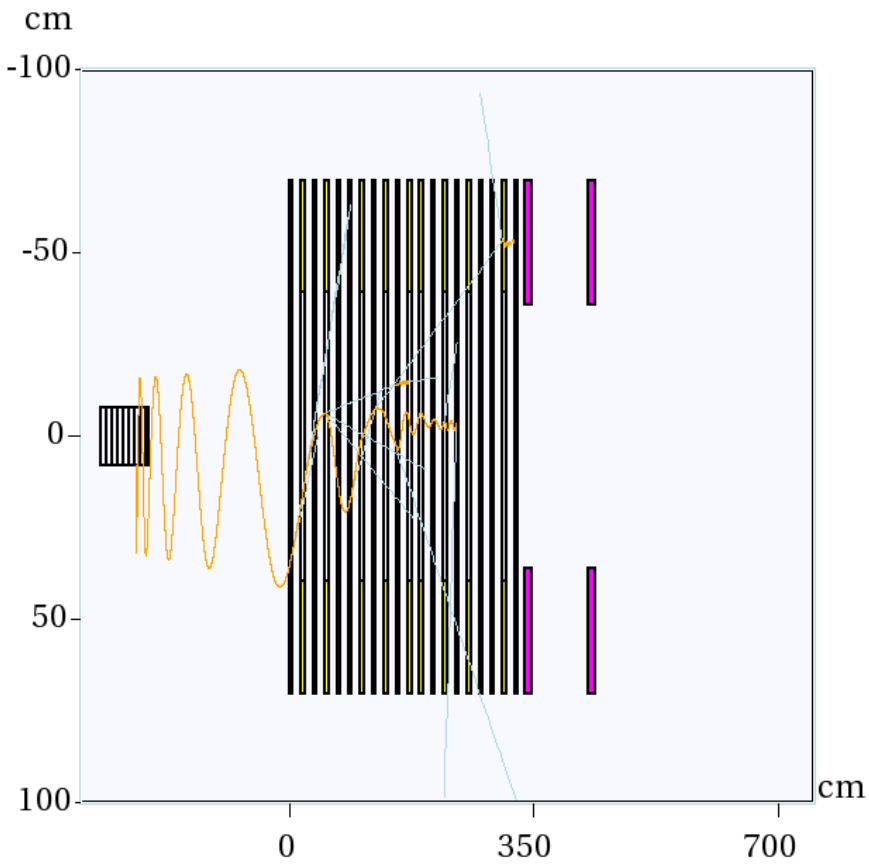

FIG. 22: Key for particles in MARS

ID	Name	Modify	Reset	ID	Name	Modify	Reset	ID	Name	Modify	Reset
1(on)	p			10(on)	e-			19(on)	nuam		
2(on)	n			11(on)	e+			20(on)	nue		
3(on)	pi+			12(on)	pbar			21(on)	nuae		
4(on)	pi-			13(on)	pi0			22(on)	K0		
5(on)	K+			14(on)	d			23(on)	nbar		
6(on)	K-			15(on)	t			24(on)	neu-hyp		
7(on)	mu+			16(on)	He3			25(on)	ch-hyp		
8(on)	mu-			17(on)	He4			26(on)	HI		
9(on)	gamma			18(on)	num				Reset All	Close	

Then we implemented the simple tracker and calorimeter design in the full existing MARS model and sent a single electron through to confirm that we observed the particle to travel through the detector as it should, which it did. Note that the particle does not trend in a downward slope along the y axis as in the toy model, this confirms what was stated earlier about the magnetic field being skewed in the toy model.

FIG. 23: Mu2e full model, observing a 105 MeV electron sent from stopping target. XZ dir.

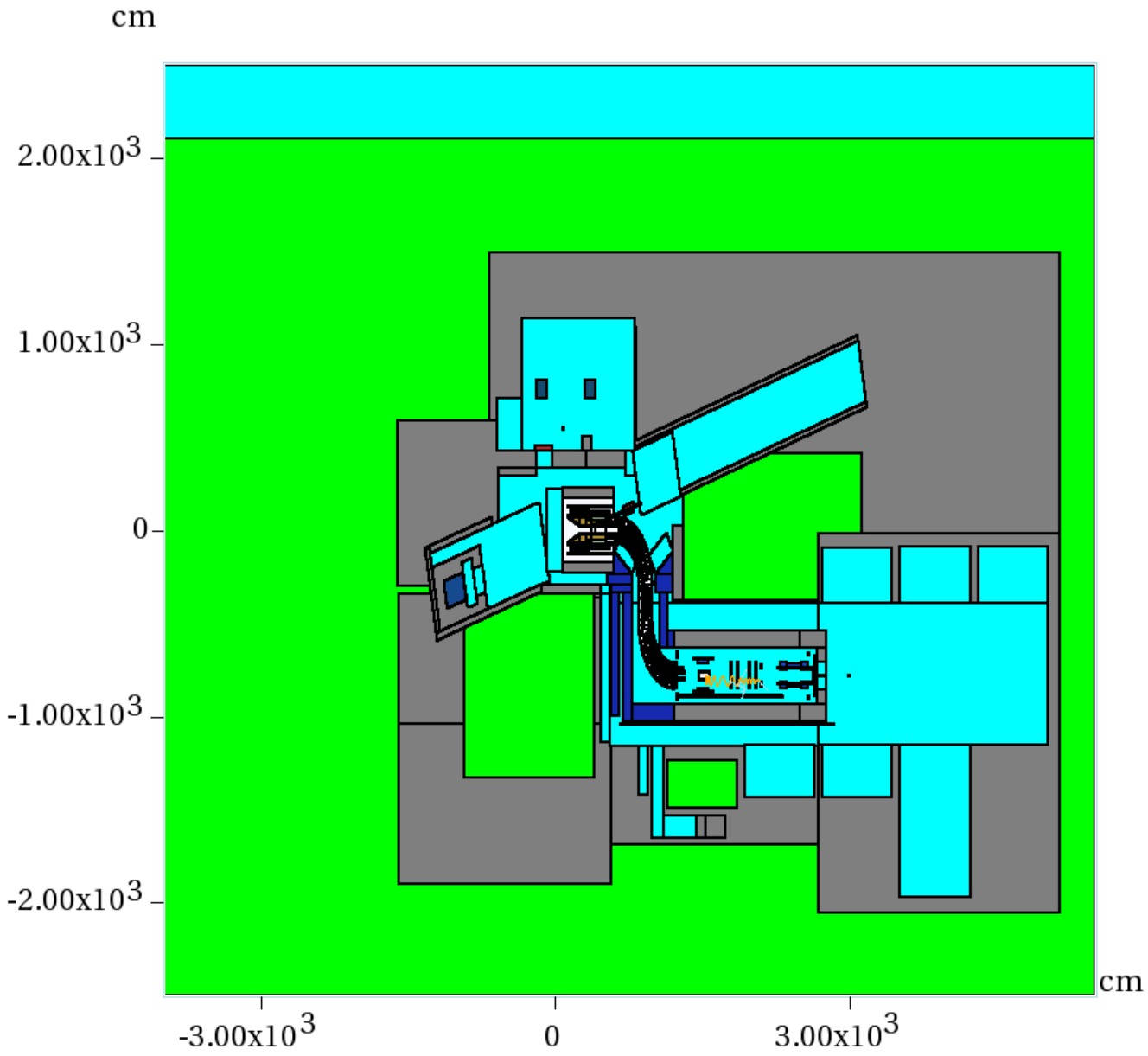

FIG. 24: 105 MeV moving from stopping target through tracker and reaching first calorimeter. (Full MARS model, single electron simulation) Initial energy: E_o = 105 MeV, initial direction cosines: $\alpha = 0$, $\beta = 1$, $\gamma = 0$ (XZ dir.)

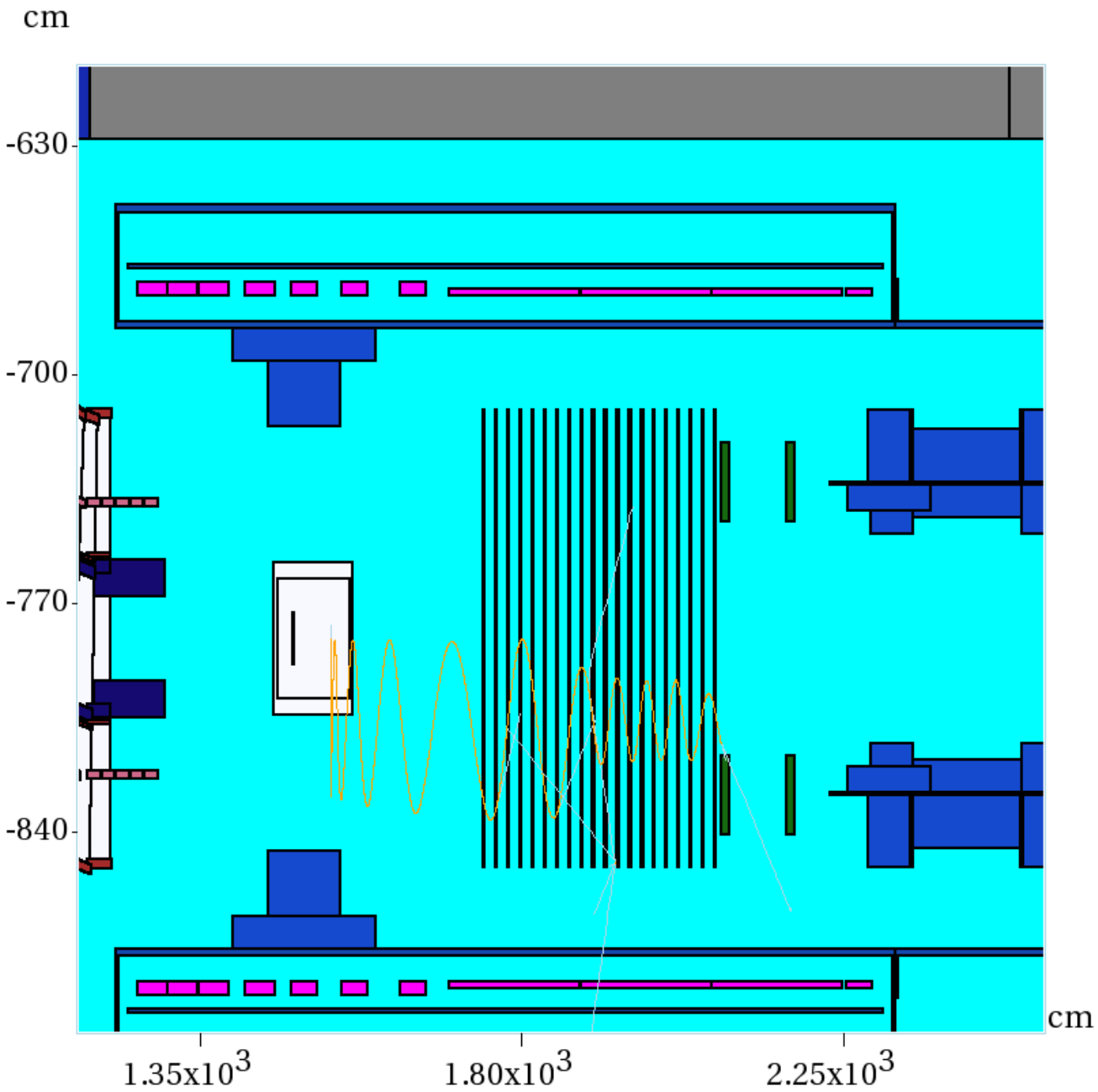

FIG. 25: 105 MeV electron moving through tracker and reaching first calorimeter. (XZ dir.)

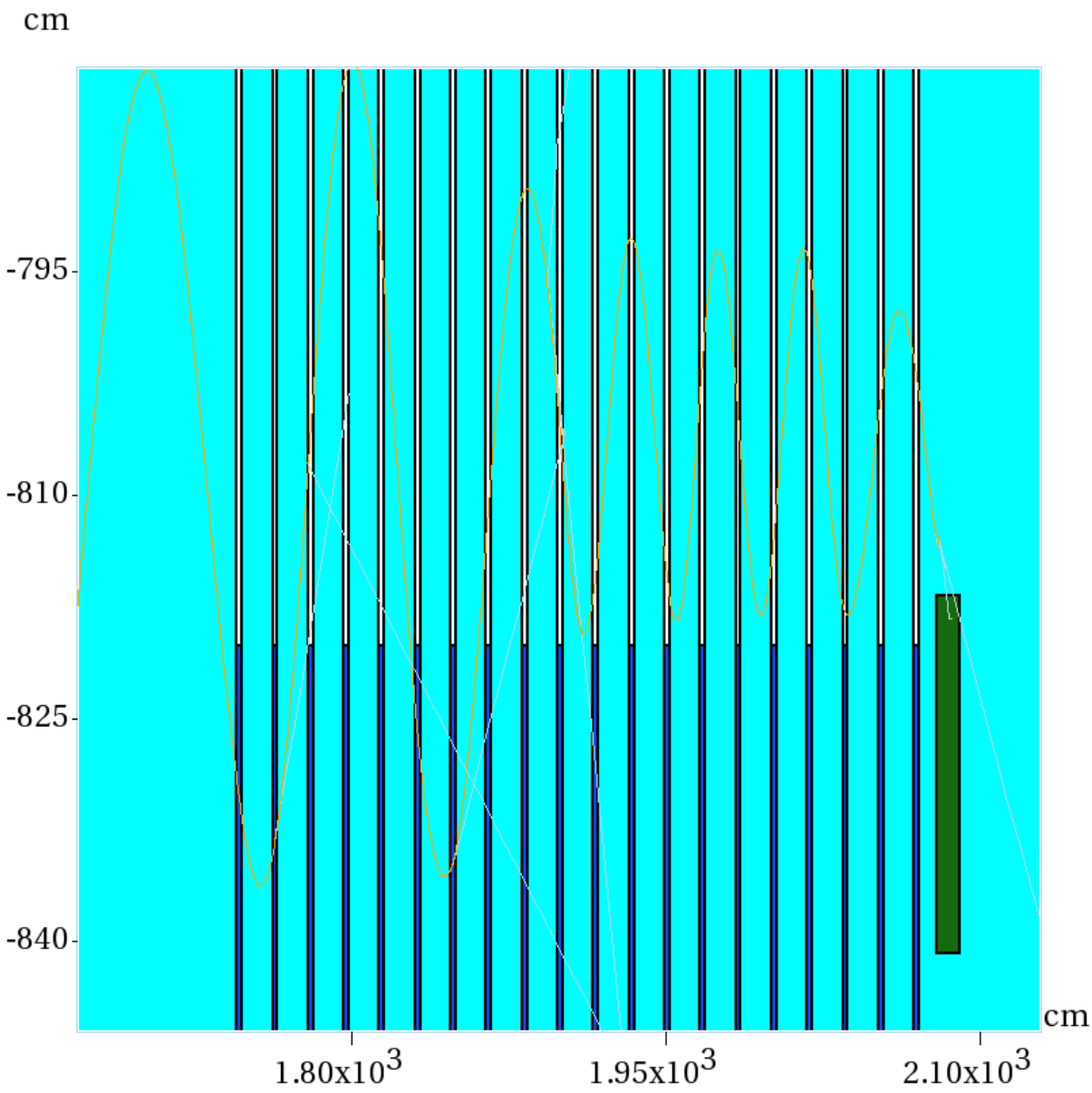

FIG. 26: Electron (orange) scattering into a photon (blue) and electron [LEFT].

FIG. 27: Diagram of the Compton effect which is what is observed in the scattering of the electron in figure 26 resulting in a decrease in energy and the emitting of a photon [RIGHT].

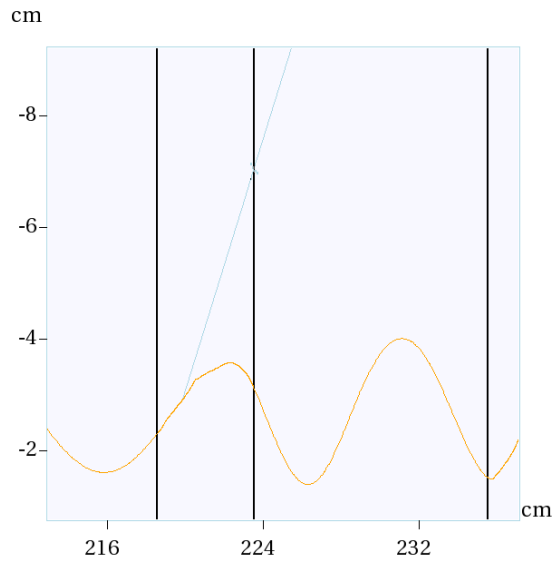

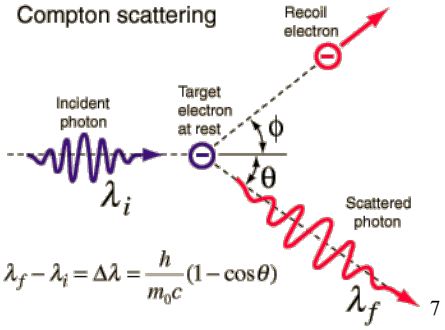

B. Mars model full simulation: Results

It takes approximately three days to run the full simulation of particles through the MARS model of the Mu2e experiment. The specs for the full simulation are: 1000 events per job, and 2500 jobs were performed at Fermigrid. The total protons on target (POT) are $2.5 * 10^6$. One must state from the get go, that the Mu2e experiment needs POT = $3.6 * 10^{20}$. Therefore, this simulation run is about only a third of the particles needed, and implies that more study in MARS will need to be done to have enough simulation data for analysis. The main results we will be looking at are energy limit cross sections of particle interactions, and the deposits of energy in histograms overlaid on the geometry of the tracker and calorimeter produced by MARS. We want to know the energy of the particles we see interact because the conversion

electron energy is 105 MeV and is like a signature to find the conversion electron. Also, we want to see the energy deposited into the materials in order to know that the materials to acquire data for the experiment will not decompose in the duration needed.

1. Energy limit cross sections : Results from MARS simulation with code built and implemented

FIG. 29: Spectrum Energy limit for an electron before entering the tracker: E limit = 107.6 MeV

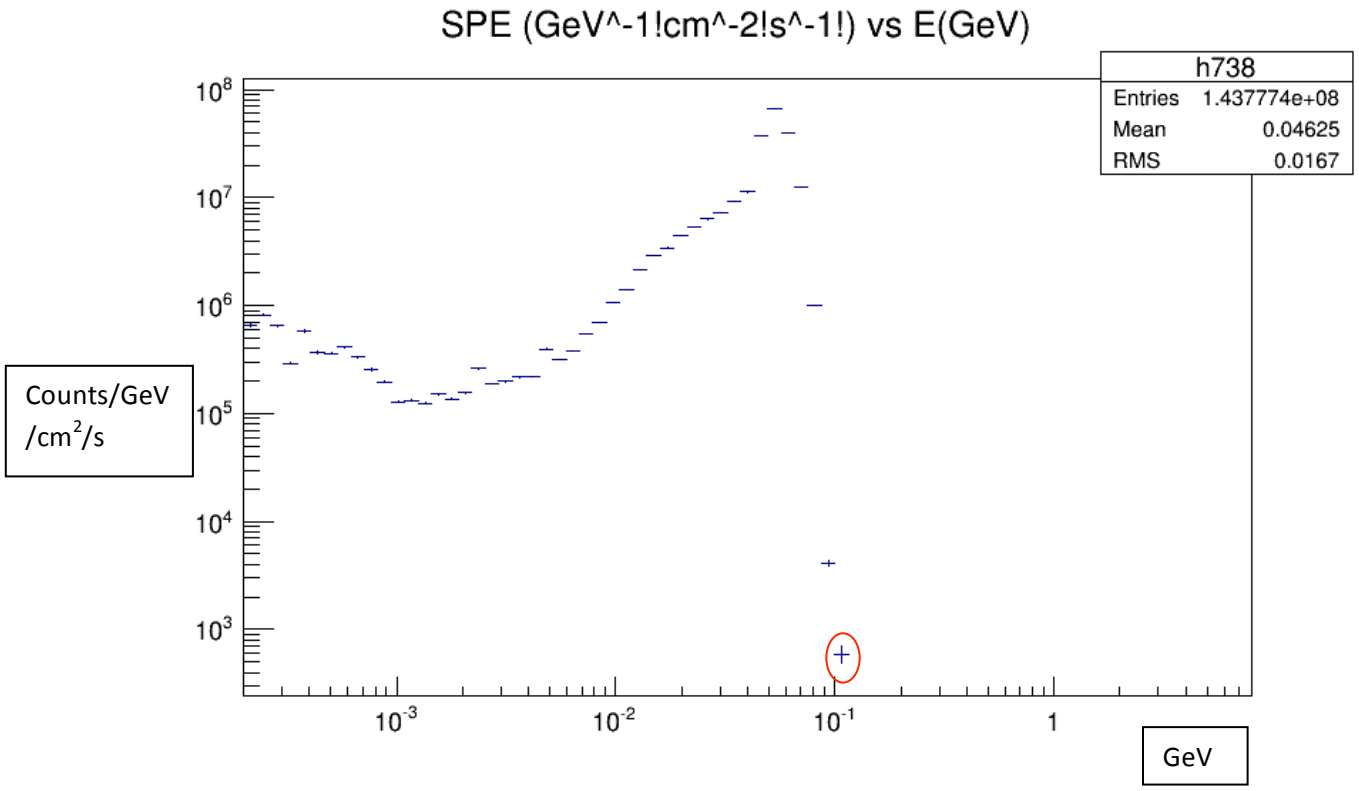

As one can see, the tracker observes an electron with about 105 MeV, the electron energy found at the limit is in fact 107.6 MeV; this is most likely a source of background such as DIO because the MARS code is not programmed for the neutrino-less conversion from a muon into an electron (either way the information is still useful to study DIO)

FIG. 30: Energy limit for electrons between the tracker and the calorimeter E limit = 123.0 MeV

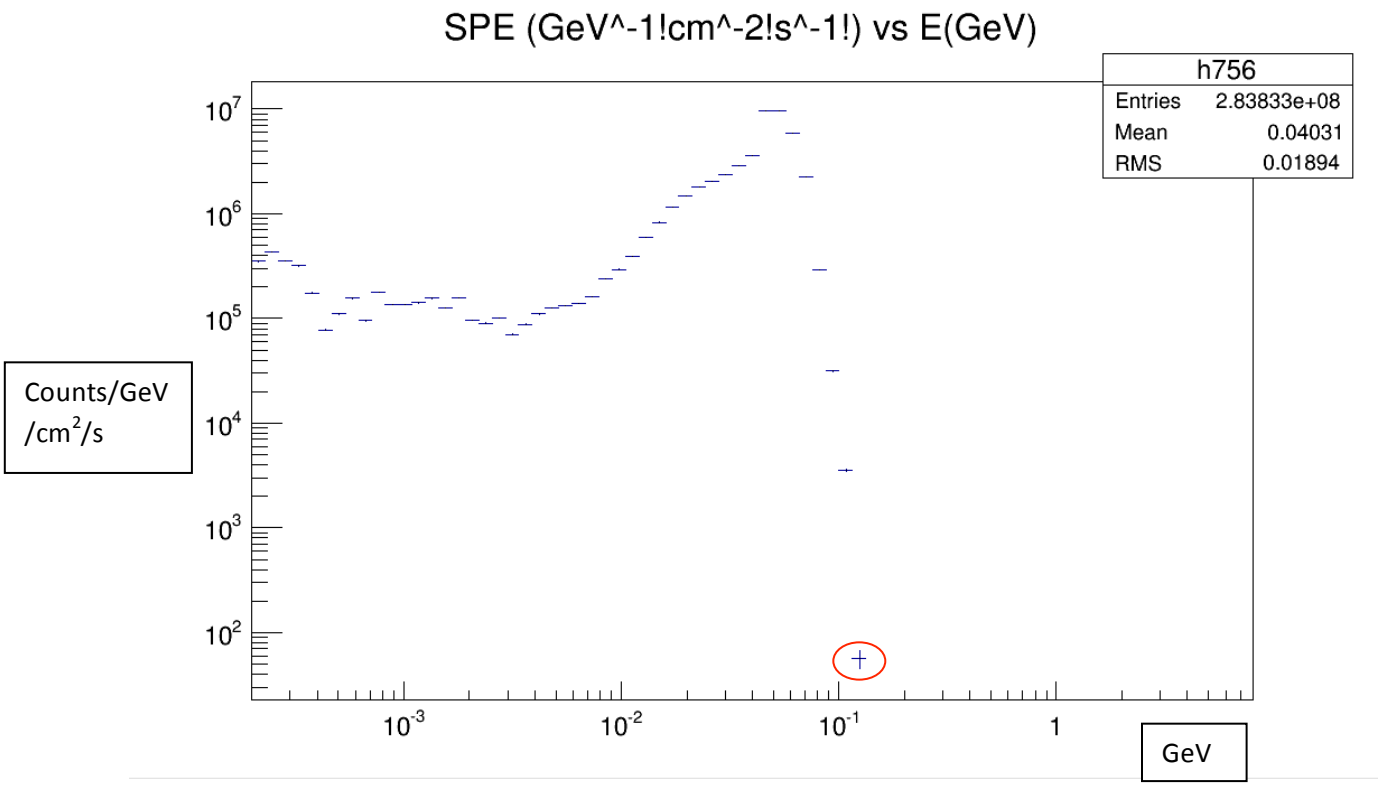

This is the energy cross section spectra taken for electrons between the tracker and the calorimeter. The energy limit is found to be 123.9 MeV, also this same energy limit was found after the calorimeter reading. At first this sounds like an error because how could energy increase while particles are decreasing? In the full simulation the working time window was not set up, therefore the electrons we are seeing here are produced by the beam flash and are most likely DIF background. Usually DIF will be mitigated by working in the correct time window as mentioned earlier; it is interesting never the less to see the proportion of DIF to DIO backgrounds in this simulation and compare it to what is predicted in the CDR.

FIG. 31:The energy limit for photons are found to be 82.7 MeV

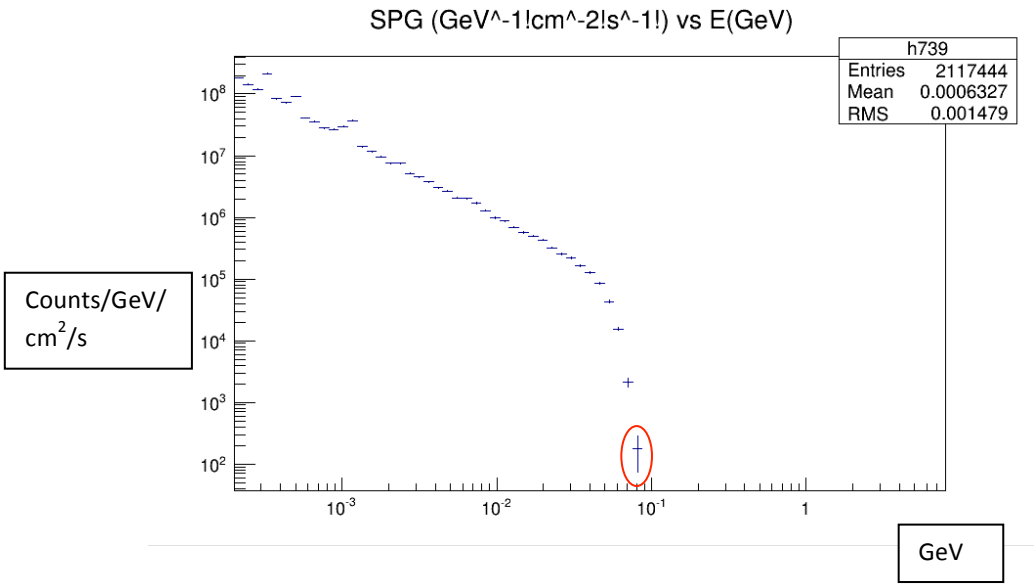

FIG. 32: Energy limit for protons before entrance to the tracker is found to be 28.9 MeV (below)

The energy limit for protons between the tracker and calorimeter is also found to be 28.8 MeV, implying that the particles are not interacting with the tracker.

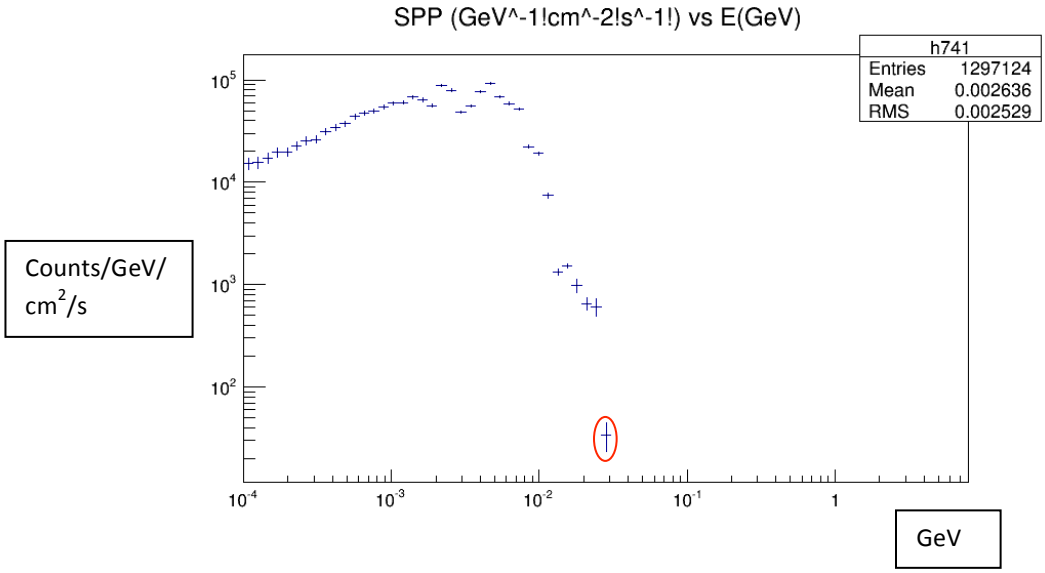

FIG. 33: The energy limit for neutrons is found to be 71.2 MeV before the tracker (shown in figure), after the tracker is found to be 71.2 MeV, and after the calorimeter is 39.5 MeV.

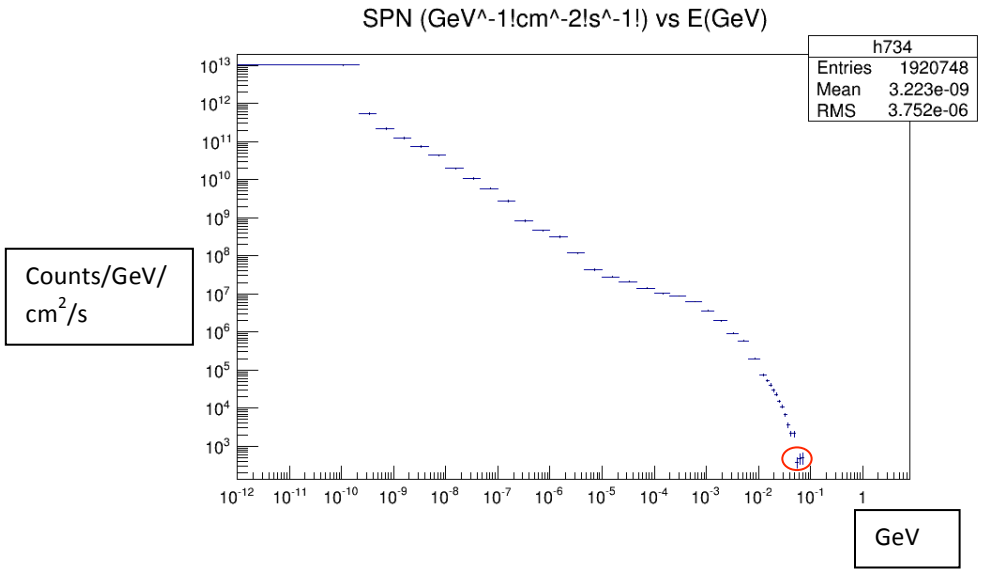

FIG. 34: Results from MARS full simulation with code built and implementation (below)

The energy limit for muons before entering the tracker is found to be 51.9 MeV.

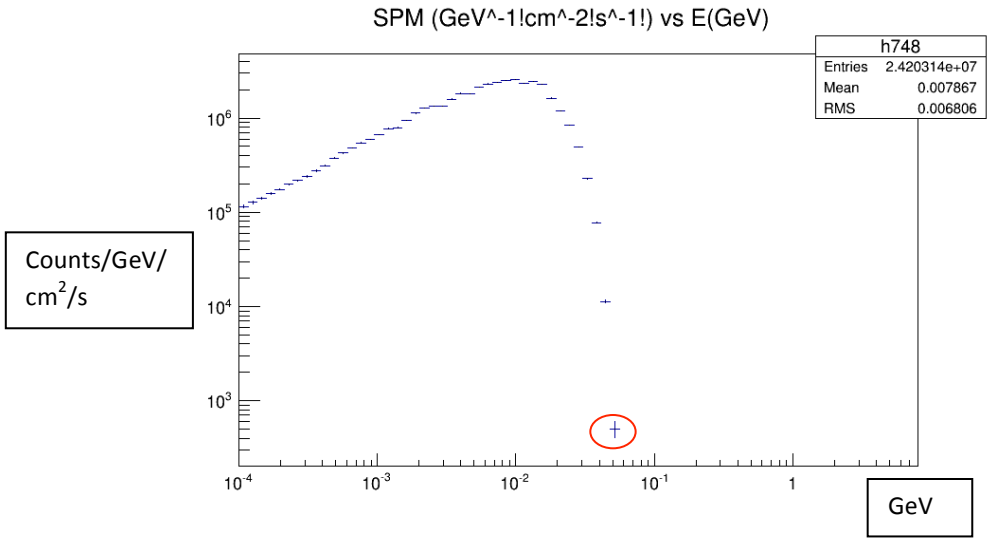

The energy limits for particles other than electrons found in the simulation are less than the conversion energy of 105 MeV. The electron energy of 107 MeV is most likely DIO, while the energy of 123 MeV for electrons found after the tracker, are hypothesized to be most likely contribution from beam flash and DIF due to not setting up the working time window before full simulation. Overall the energy limits found for particles excluding electrons are all lower than the CE. This validates the intentional geometrical design of the tracker and calorimeter, ideally they will ignore particles with less than the CE.

2. Power deposition histograms overlaying geometry

Please note that in the full simulation the tracker I built was surrounded by a general vacuum, but the existing detector solenoid in MARS was filled with air. The tracker was placed in the air. Therefore when you look at these histograms, you will notice that there is a high flux of particles in the center of the tracker and calorimeter, this is because there was air in the detector solenoid during the full simulation run.

FIG. 35: Power Deposition in Tracker (PDT)

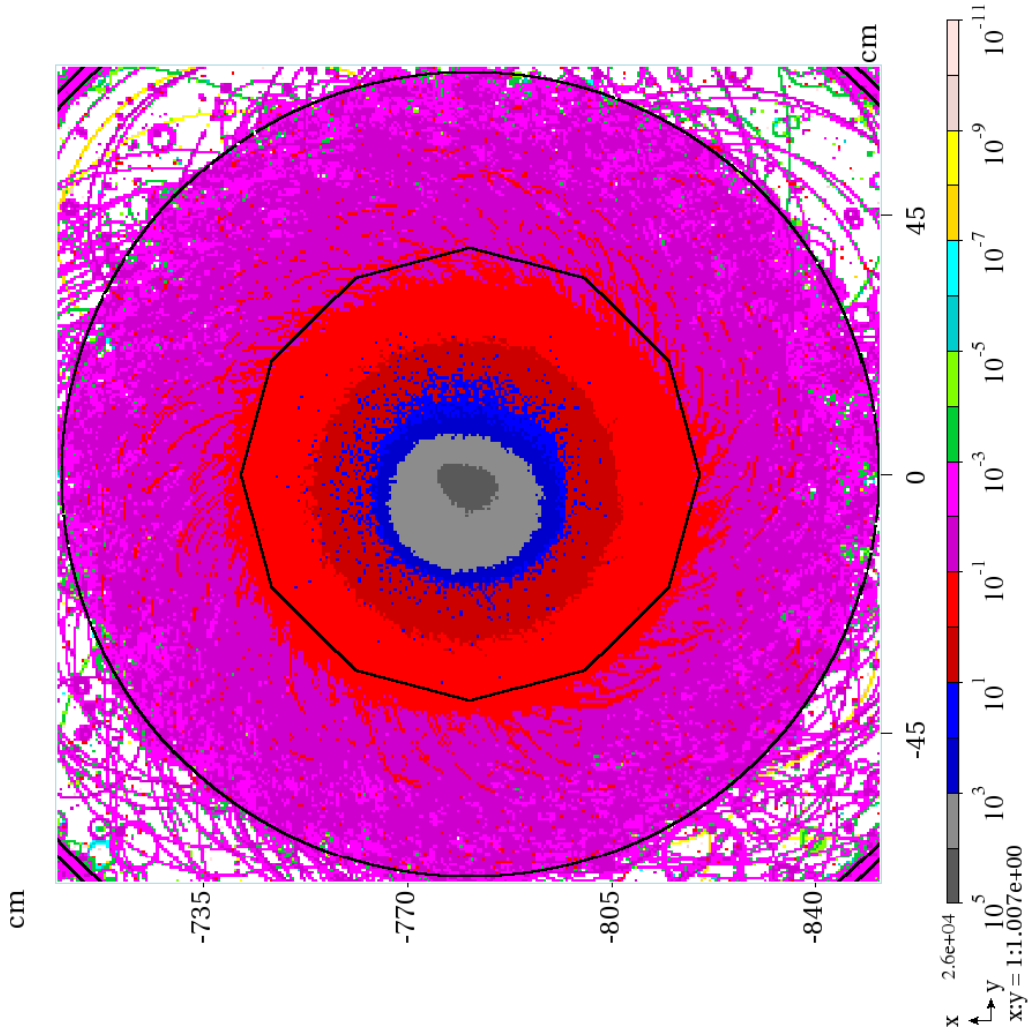

The average dose rate for the tracker is determined from an output file in MARS to be 3.97 kRad/year. Using the MARS graphical user interface (GUI) one can click with the cursor on a point of interest on the tracker and attempt to find the peak dose (PD) rate; this was done and the peak dose rate was found to be 25 kRad/year. This peak dose rate is a VERY rough approximation because when using the GUI, one tries to click on an area that looks to have the

highest power deposition, say one chooses a blue spot, but one can find also a blue spot on the calorimeter. Does this mean they both have the same peak dose rate? I don't think so.

FIG. 36: Calorimeter disk 1 PDT histogram.

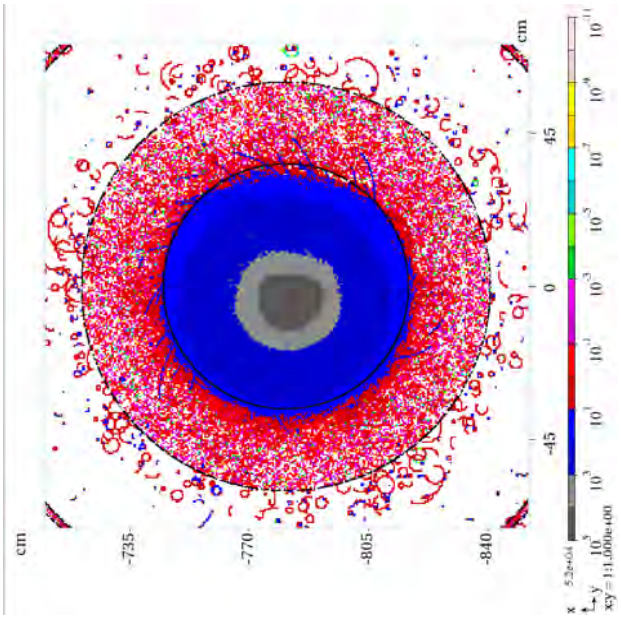

FIG. 37: Calorimeter disk 2 PDT histogram.

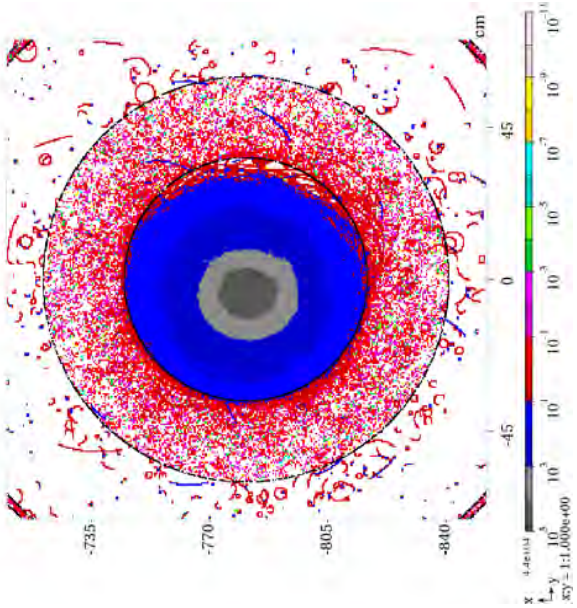

These histograms state that for the first disk, there is an average power deposition, also known as dose rate of 2.55 kRad/yr, while the second disk yields an average dose rate of 1.31 kRad/yr. The peak dose rate for the first disk is found to be approximately 22 kRad/yr, while the second disk has a peak dose rate of approximately 18 kRad/yr. There is reason to believe that the LYSO crystals are able to handle this amount of energy, although long-term periods need to be still studied.[5]

FIG. 38: Power Deposition Electrons (PDE)

Tracker (T) Calorimeter disk1(C1) Calorimeter disk2 (C2)

PD: T = 17kRad/year PD: C1 = 15kRad/year PD: C2 = 11kRad/year

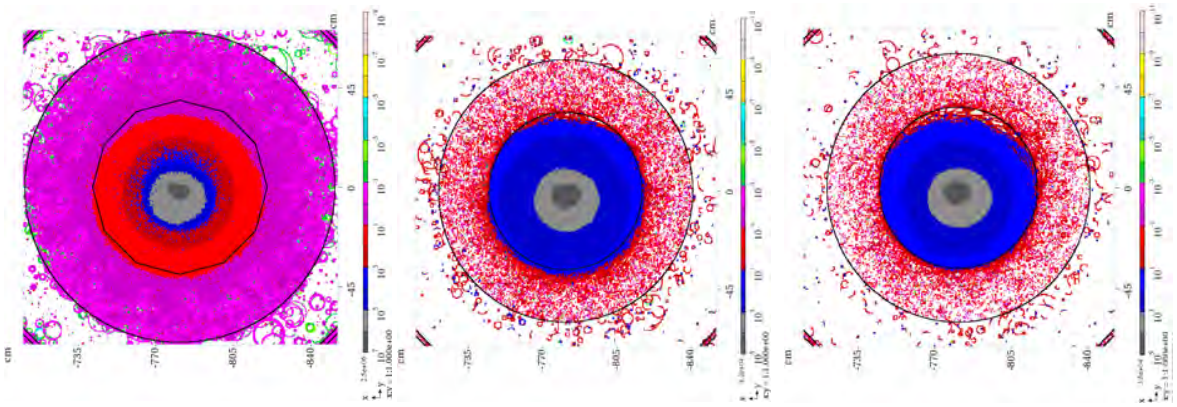

FIG. 39: Power Deposition Neutrons (PDN)

PD: T = 6.3 kRad/yr PD: C1 = 4.8 kRad/yr PD: C2 = 1.1 kRad/year

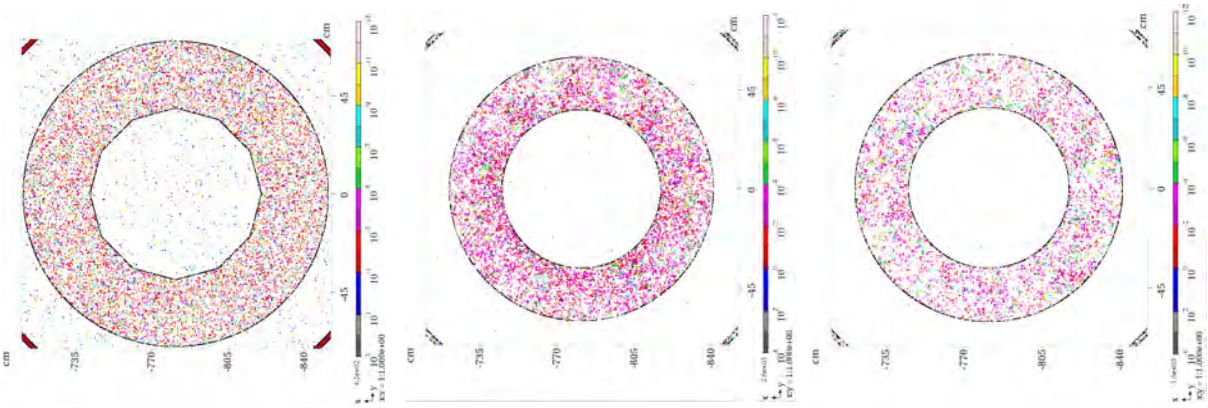

FIG. 40: Average PDT on each station of the tracker with data from MARS file

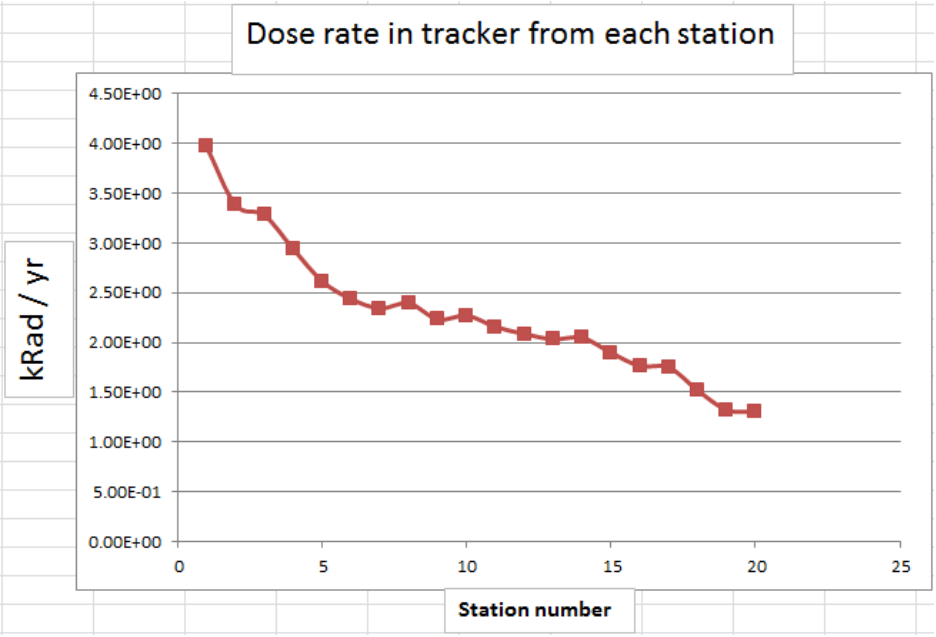

All panels are accounted for in this plot, and we can see the downward trend overall of energy deposited in the stations of the tracker is what we expect.

It will be important to note as pointed out by George G. in the simulation meeting of August 6, 2014, that there is an asymmetry observed in the power deposition histograms, which are clearly visible in the PDT and PDE histograms. The histograms show a trend to spill over onto one side of the tracker and calorimeter more than the other, in the direction of the figures this is the bottom and slightly left (if looking at it head on) inner radius portion of the geometry. This asymmetry, also brought up in the simulation meeting, is usually what is found to happen in experiments. This may be due to the magnetic field and the gradient functions that were inputted. It is interesting to note that in the toy MARS model I observed single particles trending downwards in the –x or -y direction based on the direction cosine input into MARS.INP, and here, in the full simulation with the pre-existing magnetic field code, there is a slightly overall

greater particle and thus energy distribution in the negative y direction, when the direction cosines for the full MARS run was $\alpha = 1$, $\beta = 0$, $\gamma = 0$. This points to the dependency of uneven distribution based upon the angles that the particles are emitted from the stopping target.

VI. CONCLUSION

Direct simulations in MARS are successfully used with the models I built of the tracker and calorimeter programmed in ROOT. The results from the toy simulation find that the geometry of the tracker should ignore electrons with energy less than the 105 MeV of the conversion electron, but if the magnetic field is not precisely uniform, and the particle is sent in uneven direction cosines, the possibility of an electron with as low energy as 60 MeV can intersect the tracker and be a source of background. In the full simulation, it is interesting that a cross section of energy of approximately 105 MeV was observed. This is most likely from decay in orbit background, or may even point to an explanation not yet formulated. From the power deposition histograms, the calorimeter has an average dose rate of 2.55 kRad/yr for the front disk and 1.31 kRad/yr for the back disk. This data can be compared to B. Echenard, and G.Pezullo's presentation in June 2014 where they found an average dose rate of 3 kRad/yr for the front disk and 0.5 kRad/yr for the back disk. Which is a -15% difference for the first disk and +38 % difference for the back disk. More study should be done to investigate the difference of these models and the details of the models used in the simulations. When comparing the peak dose rate (which is in itself a very rough approximate due to the data being obtained from the MARS GUI) electrons contribute to approximately 68% of the total PDT (average), while neutrons contribute to approximately 15.6% to total average PDT. Mu2e finding CLFV at a rate beyond the Standard Model will provide us with a deeper understanding of particles, their interaction, and their

relationships. This understanding is crucial for the future of physics to develop the theories that underlie our reality.

VII. ACKNOWLEDGEMENTS

I would like to thank Vitaly Pronskih, Nikolai Mokhov, the Mu2e collaboration, Roger Dixon, Erik Ramberg, Tanja Waltrip, Marge and Bill Bardeen, the Computing Service Desk, SULI, and Fermilab. This work was supported in part by the U.S. Department of Energy, Office of Science, and Office of Workforce Development for Teachers and Scientists (WDTS) under the Science Undergraduate Laboratory Internships Program (SULI)

VIII. APPENDIX

A. The source code for the trapezoidal geometry tracker in ROOT, MARS toy model (file name: tgeo_init.cc)

```
#include <iostream>
#include <sstream>
#include <string.h>
#include <stdlib.h>
#include <map>
#include "TROOT.h"
#include "TMath.h"
#include "TGeoManager.h"
#include "TGeoMedium.h"
#include "TGeoMaterial.h"
#include "TGeoTube.h"
#include "TGeoPgon.h"
#include "TGeoTrd1.h"
#include "TGeoVolume.h"
#include "TGeoMatrix.h"
#include "TGeoCompositeShape.h"

static const   Double_t Zmax=750.0; // cm
static const   Double_t Rmax = 100.0;    // cm

extern "C" {
  void tgeo_init_()
  {

    ////////////////////tracker design with trapezoidal panels/////////////////////////////////////
    Int_t i;
    TGeoMedium* GVAC = gGeoManager->GetMedium(2);
    TGeoMedium* AL = gGeoManager->GetMedium("AL");
    TGeoMedium* MIX1 = gGeoManager->GetMedium(3);
    TGeoMedium* LYSO = gGeoManager->GetMedium("LYSO");

    TGeoVolume* World = gGeoManager->MakeTube("WORLD",GVAC,0,Rmax,Zmax);
    TGeoVolume *plane = new TGeoVolumeAssembly("PLANE");

    Double_t xplatebot = 30*2;
    Double_t xplatetop = 8.5*2;
    Double_t zplate = 7.65*2;
    Double_t dshift = 25*2;

    TGeoVolume *trap = gGeoManager->MakeTrd1("TRAP",MIX1,xplatebot, xplatetop,.5,zplate);
    TGeoVolume *slice1 = trap->Divide("SLICE1",3,25,0,0);
    TGeoVolume *slice2 = slice1->Divide("SLICE2",2,2,0,0);
    slice1->SetLineColor(kBlue);
    slice2->SetLineColor(kBlue);

    plane->AddNode(trap,1);

    TGeoRotation *rot1 = new TGeoRotation();
    rot1->RotateX(90);
    TGeoRotation *rot;
    TGeoVolume *panel = new TGeoVolumeAssembly("PANEL");
    for(i=0; i<3; i++)
      {
      Double_t phi = 120.*i;
      Double_t phirad = phi*TMath::DegToRad();
      Double_t xp = dshift*TMath::Sin(phirad);
      Double_t yp = -dshift*TMath::Cos(phirad);
      rot= new TGeoRotation(*rot1);
      rot->RotateZ(phi);
      panel->AddNode(plane,i+1,new TGeoCombiTrans(xp,yp,0,rot));
      }
```

```
TGeoVolume *outerTube = gGeoManager->MakeTube("OUTERTUBE", GVAC,0,70,.5);
outerTube->SetLineColor(kBlue);
outerTube->AddNode(panel,1);


TGeoVolume *station = new TGeoVolumeAssembly("STATION");

Int_t ncells = 4;
Int_t j;
for(j=1; j<=ncells; j++)
  {

    if((j-1)==0)
    {
       Double_t zcell = (j-1)*(1);
       station->AddNode(outerTube,ncells+j+1, new TGeoTranslation(0,0,zcell));
      }
    if((j-2)==0)
    {
        TGeoRotation *rot2 = new TGeoRotation();
        rot2->RotateZ(60);
        Double_t zcell = (j-1)*(1);
        station->AddNode(outerTube,ncells+j+1, new TGeoCombiTrans(0,0,zcell,rot2));
      }
    if((j-3)==0)
    {
        TGeoRotation *rot3 = new TGeoRotation();
        rot3->RotateZ(30);
        Double_t zcell = (i-1)*(1);
        station->AddNode(outerTube, ncells+i+1, new TGeoCombiTrans(0,0,zcell,rot3));
      }

    if((j-4)==0)
    {
      TGeoRotation *rot4 = new TGeoRotation();
      rot4->RotateZ(90);
      Double_t zcell = (j-1)*(1);
      station->AddNode(outerTube, ncells+j+1, new TGeoCombiTrans(0,0,zcell,rot4));
    }

  }


Int_t nstations = 20;

for(i=0; i<nstations; i++)
{
   Double_t zstation = (i)*(18);
   World->AddNode(station,i+1, new TGeoTranslation(0,0,zstation));
  }
```

```
  TGeoVolume* calTube = gGeoManager->MakeTube("CALTUBE",LYSO,36,70,5.5);
  calTube->SetLineColor(kBlue);

  TGeoVolume* stopTar = gGeoManager->MakeTube("STOPTAR",GVAC,0,8,4);
  stopTar->SetLineColor(kBlue);



  for(i=0; i<16; i++)
    {

      World->AddNode(stopTar,i+1, new TGeoTranslation("sttr",0,0,-208-(i*4)));
       }


  World->AddNode(calTube, 1, new TGeoTranslation("ctr",0,0,338));
  World->AddNode(calTube,2, new TGeoTranslation("ctr2", 0,0,418));




      gGeoManager->SetTopVolume(World);
      gGeoManager->CloseGeometry();
      gGeoManager->Export("MyGeom.root");

  }
}
```

B. Code implemented in MARS full model, added to existing code (file name: tgeo_init.cc)

```
Int_t i;

TGeoMedium* Mix1 = gGeoManager->GetMedium(56);
TGeoMedium* LYSO = gGeoManager->GetMedium(57);

TGeoVolume* outerTube = gGeoManager->MakeTube("OUTERTUBE",Mix1,0.,70,1.25);

TGeoVolume* poly2 = gGeoManager->MakePgon("POLY2",GVAC,0,360,12,2);
TGeoPgon* pgon2 = (TGeoPgon*)(poly2->GetShape());
pgon2->DefineSection(0,-1.25,0,38);
pgon2->DefineSection(1,1.25,0,38);

outerTube->AddNode(poly2,1);
outerTube->SetLineColor(kRed);


Int_t ncells = 20;
for(i=0; i<ncells; i++) {

Double_t zcell =(i)*(17);

World->AddNode(outerTube,(i+1), new TGeoTranslation("wtr",0,-780.8,1745.9+zcell));
     }

  TGeoVolume* calTube1 = gGeoManager->MakeTube("CALTUBE1",LYSO,36,70,5.5);
  calTube1->SetLineColor(kRed);

  TGeoVolume* calTube2 = gGeoManager->MakeTube("CALTUBE2", LYSO,36,60,5.5);
  calTube2->SetLineColor(kRed);

  //TGeoVolume* stopTar = gGeoManager->MakeTube("STOPTAR",AL,0,8,4);
  //stopTar->SetLineColor(kBlue);


  //      for(i=0; i<16; i++) {

  //        World->AddNode(stopTar,i+1, new TGeoTranslation("sttr",0,0,-208-(i*4)));
  //                       }


World->AddNode(calTube1, 1, new TGeoTranslation("ctr1",0,-780.8,2083.9));
World->AddNode(calTube2,1, new TGeoTranslation("ctr2",0,-780.8,2174.9));
```

C. B field subroutine added to Fortran MARS toy model (file name m1514.f)

```
BY1 = ZRO
BY2 = ZRO
BY3 = ZRO

BZ1 = ZRO
BZ2 = ZRO

XCURR = X*10.d0 - 3904.d0
YCURR = Y*10.d0
ZCURR = Z*10.d0 + 8146.d0

IF(XCURR.GE.-3904.D0) THEN
   XCURR = -3904.D0-(XCURR + 3904.D0)
   XSIGN= 1.d0
   else
      XSIGN=-1.d0
END IF

BX1 = 3.67853d-7*(XCURR**2.)
BX2 = 0.00296199*XCURR
BX3 = 5.97036

BX = (BX1+BX2+BX3)*XSIGN

IF (YCURR.LE.0.D0) THEN
   YCURR=ABS(YCURR)
   YSIGN=-1.d0
   else
      YSIGN=1.d0
END IF

BY1 = 6.83929d-8*(YCURR**2.)
BY2 = 9.80995d-5*YCURR
BY3 = 0.00187768

BY = (BY1 + BY2 +BY3)*YSIGN

IF (ZCURR.LE.8146.D0) THEN
       BZ1= -0.00025719*ZCURR
       BZ2 = 2.99841D0

       ELSE

          BZ1 = 1.D0
          BZ2 = 0.D0

       END IF

       BZ = BZ1 + BZ2

BBB = SQRT(BX*BX+BY*BY+BZ*BZ)
```

IX. REFERENCES

[1]Robert Bernstein. (Mu2e Collaboration) PRISM-PRIME Proposal. Mu2e Document 2202-v2. (2012).

[2]D. Glenzinki. (Mu2e Collaboration) The Mu2e Experiment at Fermilab. Mu2e Document 690-v1. PACs: 13.35.Bv, 12.15.Ff (2009).

[3]Nikolai Mokhov, and Catherine James. *The MARS Code System User's Guide*, Version 15 (2014).

[4]Mu2e CDR (2012).

[5]Jianming Chen *et al.* Large Size LSO and LYSO Crystals for Future High Energy Physics Experiments (2007).

[6]R.H. Bernstein, Peter S. Cooper. Charged Lepton Flavor Violation: An Experimenter's Guide. Physics Reports (2013).

[7]http://physics-pelago.blogspot.com